

# Growth of thin films by physical vapor deposition

Magnetic materials in nanoelectronics

- properties and fabrication



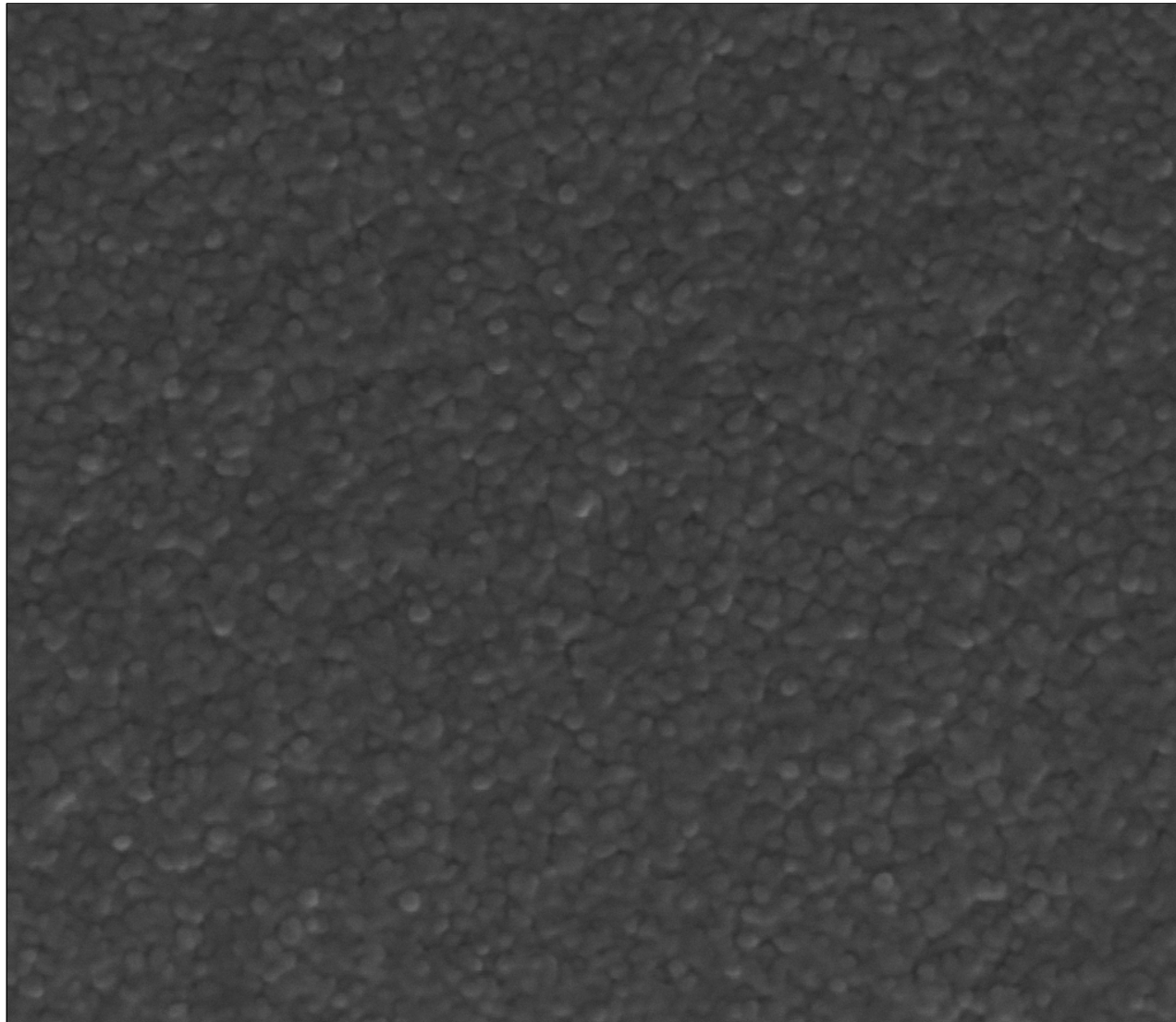
# Growth of thin films by physical vapor deposition

---

1. Introduction
2. Initial growth
3. Further stages of growth

# Introduction

In most cases the structure of the film is very different from an ideal



electron microscopy image

- the sputtered film\* consists of many sub-micrometer grains of irregular shapes

	2/12/2014	WD	HV	HFV	 500 nm NPV70/9920969
	12:14:34 PM	5.2 mm	30.00 kV	2.55 μm	

\*naturally oxidized Si(100)/Au(2 nm)/[(Co(0.6 nm)/Au(2 nm)/Py(2 nm)/Au(2 nm)]<sub>10</sub>

# Introduction

Electronic/spintronic devices can be deposited on different substrates. Some of them are:

- crystalline Si (usually from wafers [2])
- oxidized Si
- glasses
- sapphire
- MgO
- and many many others...

monocrystalline ingots made with Czochralski method



The substrates can be:

- crystalline
- polycrystalline/nanocrystalline
- amorphous

Cube made of polycrystalline Silicon

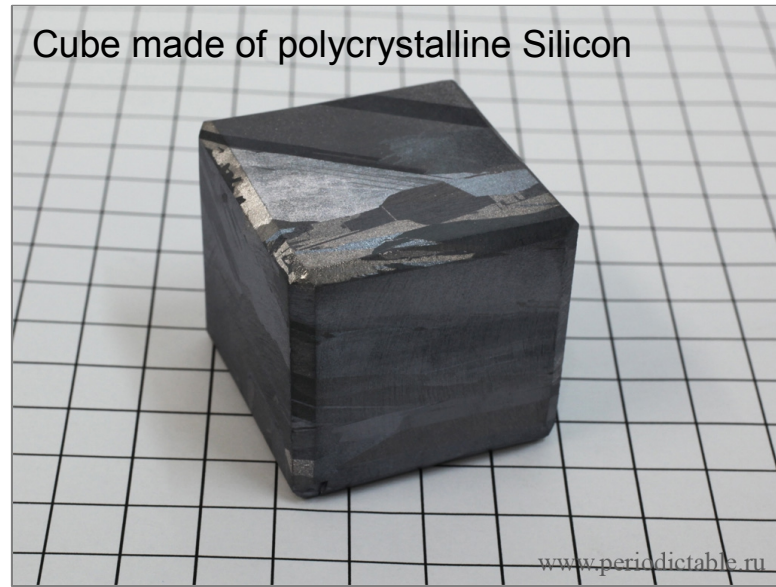
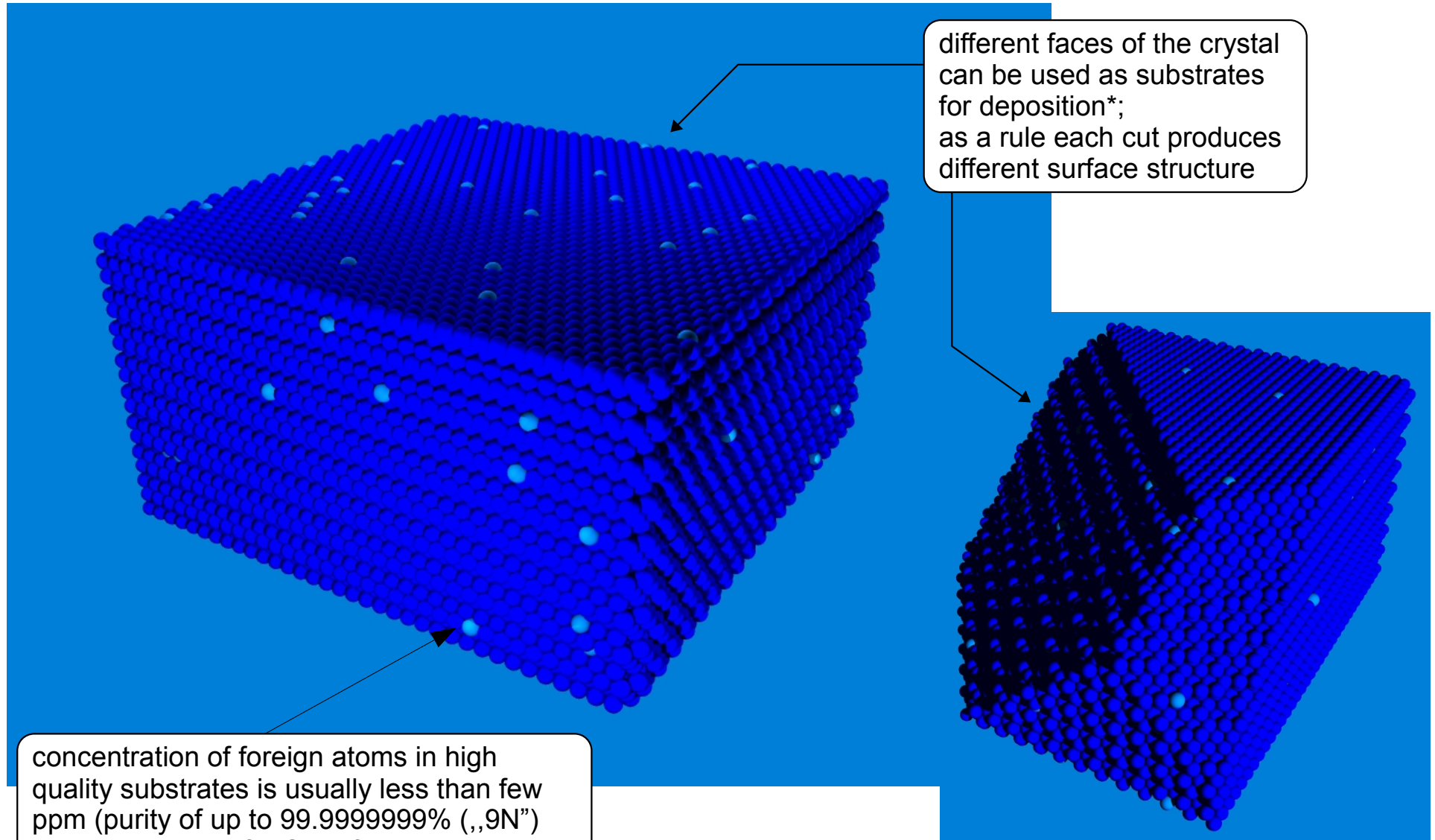


image from: [http://www.periodictable.ru/014Si/Si\\_en.html](http://www.periodictable.ru/014Si/Si_en.html)

# Introduction

Schematic of a structure a crystalline (fcc) substrate:



\*you are encouraged to visit An Introduction to Surface Chemistry by Dr. Roger M. Nix ; <http://www.chem.qmul.ac.uk/surfaces/scc/> and Surface Explorer at <http://surfexp.fhi-berlin.mpg.de/>

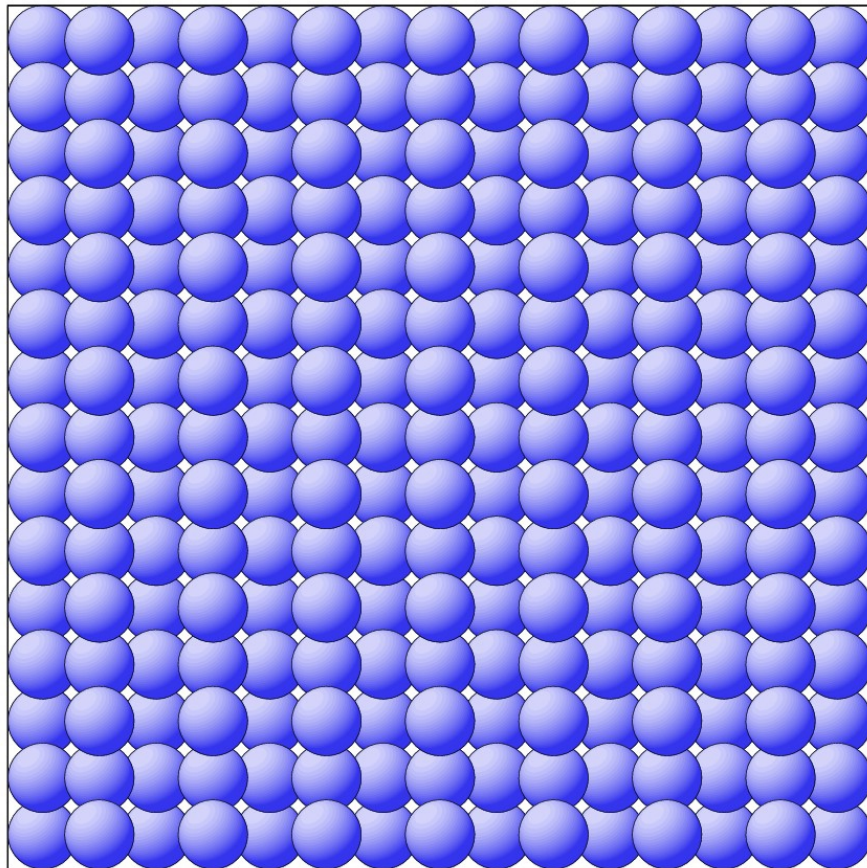
# Introduction

One of the most widely used substrates are **silicon wafers**

Depending on cut of the diamond structure (two fcc lattices shifted by  $\langle \frac{1}{4}, \frac{1}{4}, \frac{1}{4} \rangle$ ) different surfaces can be produced which influence the deposition of materials.

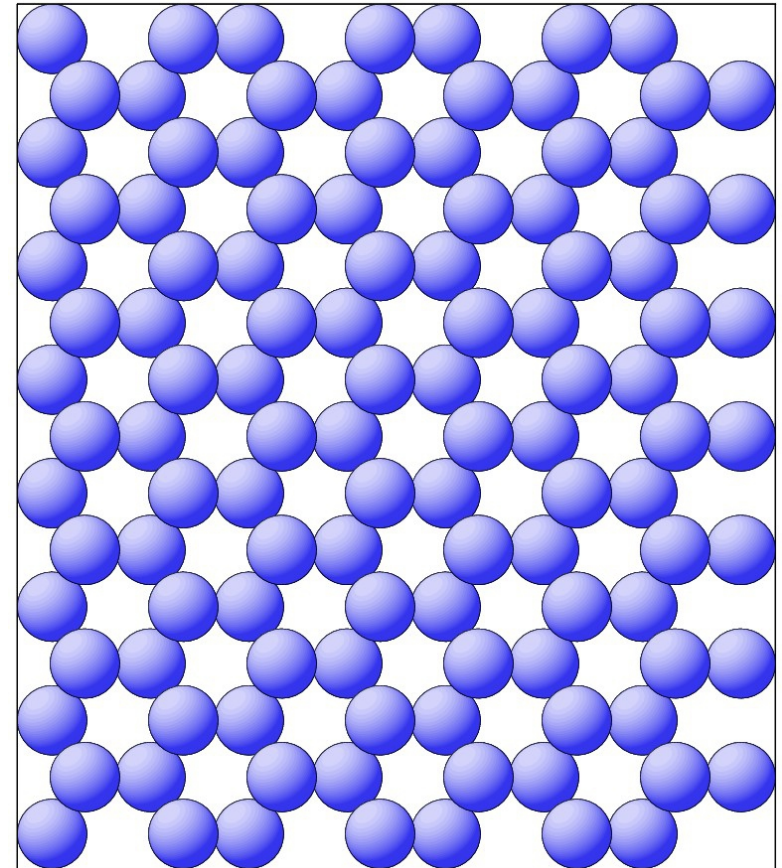
**(100)**

parallel projection, 4 layers



**(111)**

parallel projection, 4 layers



images from: Klaus Hermann, Surface Explorer at <http://surfexp.fhi-berlin.mpg.de> [(c) Balsac by K. Hermann, Fritz-Haber-Institut Berlin (Germany)]

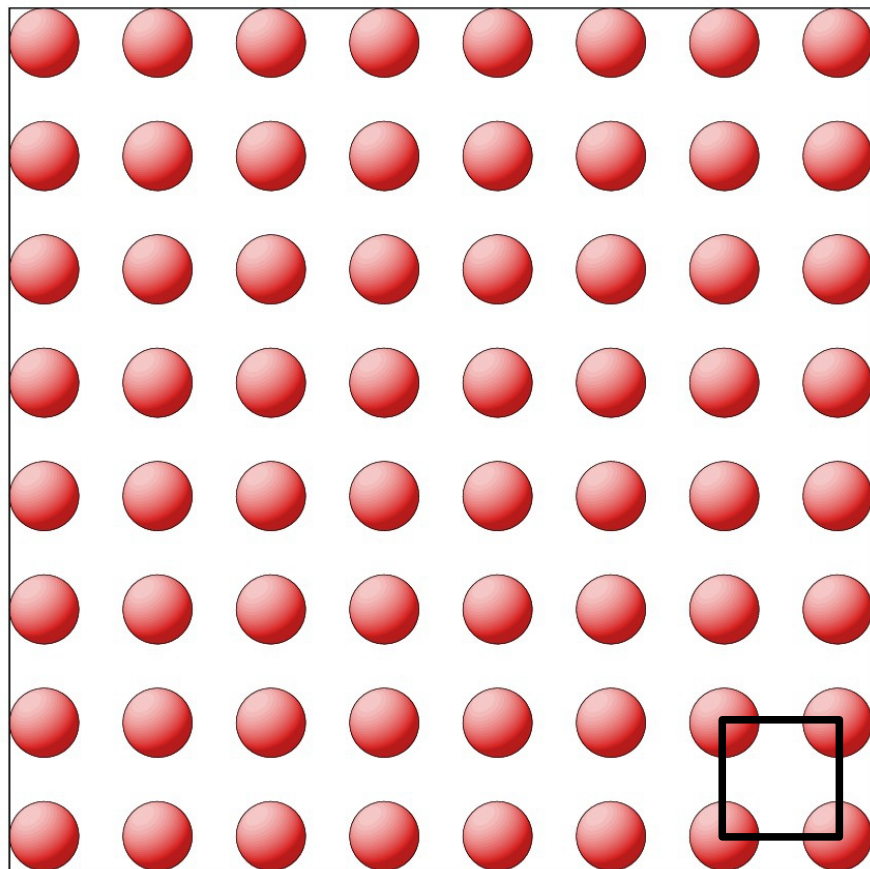
# Introduction

One of the most widely used substrates are **silicon wafers**

Depending on cut of the diamond structure (two fcc lattices shifted by  $\langle \frac{1}{4}, \frac{1}{4}, \frac{1}{4} \rangle$ ) different surfaces can be produced which influence the deposition of materials.

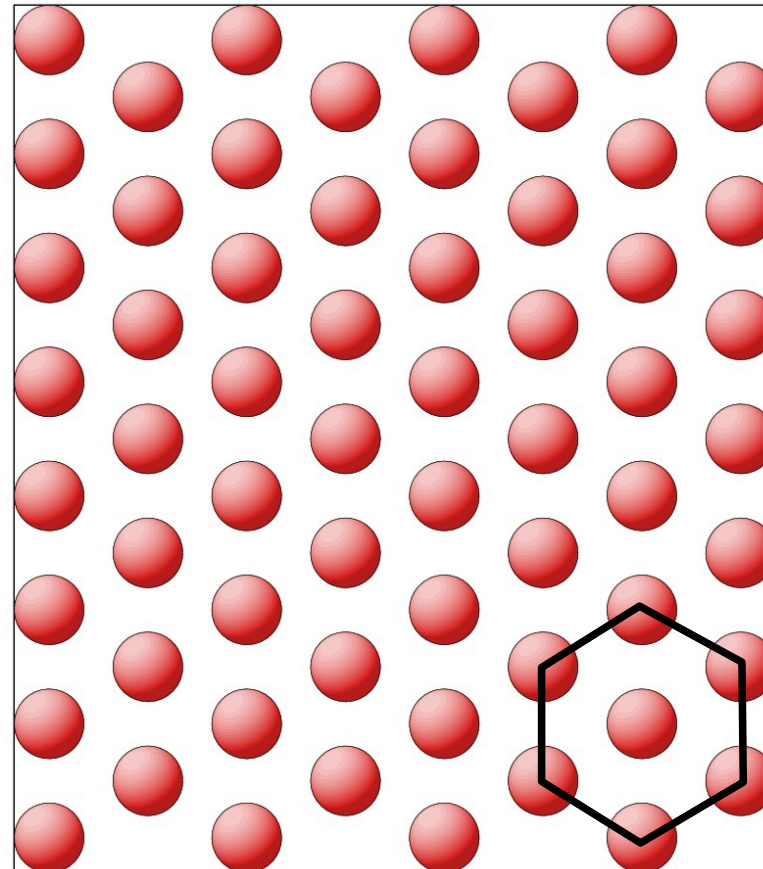
**(100)**

parallel projection, 1 layer



**(111)**

parallel projection, 1 layer



images from: Klaus Hermann, Surface Explorer at <http://surfexp.fhi-berlin.mpg.de> [(c) Balsac by K. Hermann, Fritz-Haber-Institut Berlin (Germany)]

**in-surface symmetry depends on surface orientation**

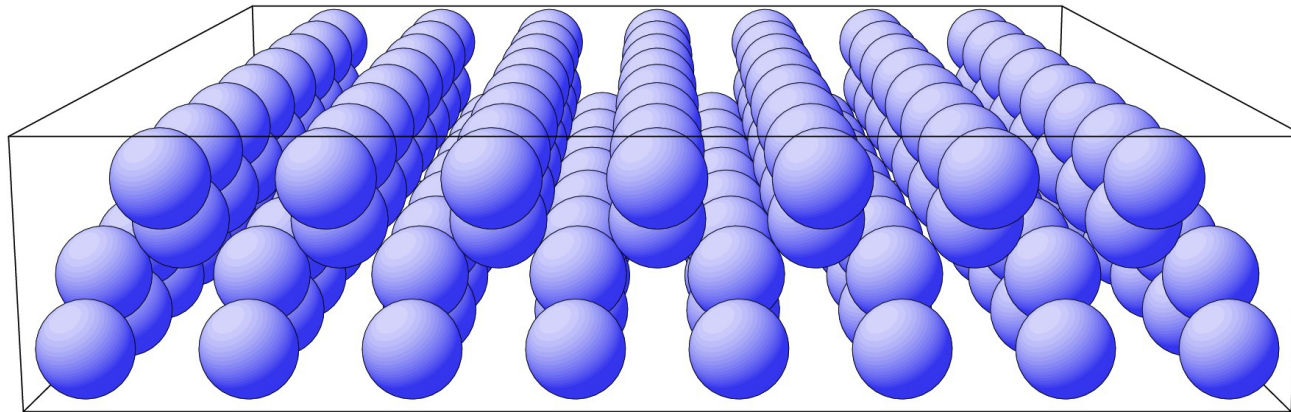
# Introduction

One of the most widely used substrates are **silicon wafers**

Depending on cut of the diamond structure (two fcc lattices shifted by  $\langle \frac{1}{4}, \frac{1}{4}, \frac{1}{4} \rangle$ ) different surfaces can be produced which influence the deposition of materials.

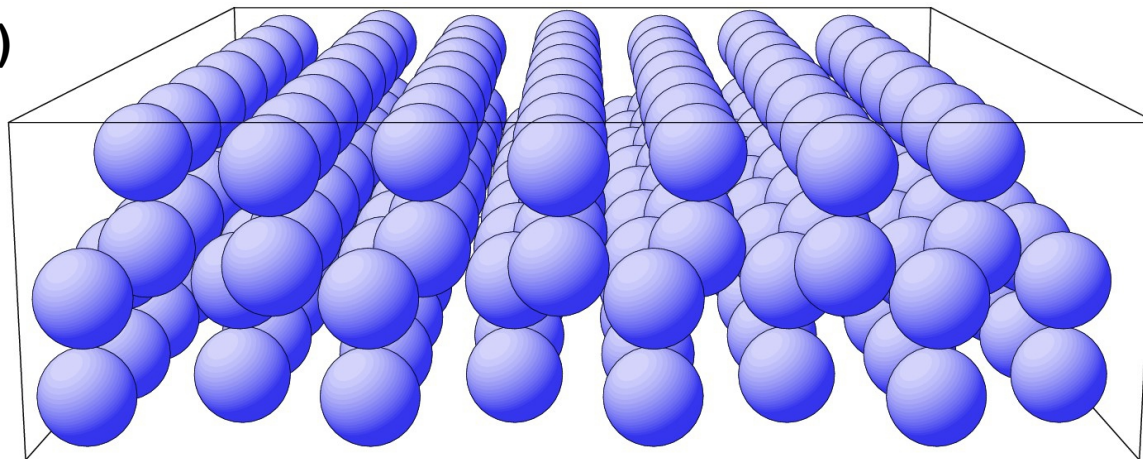
**(100)**

perspective



**(111)**

perspective



images from: Klaus Hermann, Surface Explorer at <http://surfexp.fhi-berlin.mpg.de> [(c) Balsac by K. Hermann, Fritz-Haber-Institut Berlin (Germany)]

# Introduction

When cut along certain planes many crystal structures tend to reorganize to minimize energy. Si is a notable example – the occurrence of **reconstruction** depends on temperature, foreign inclusions etc.

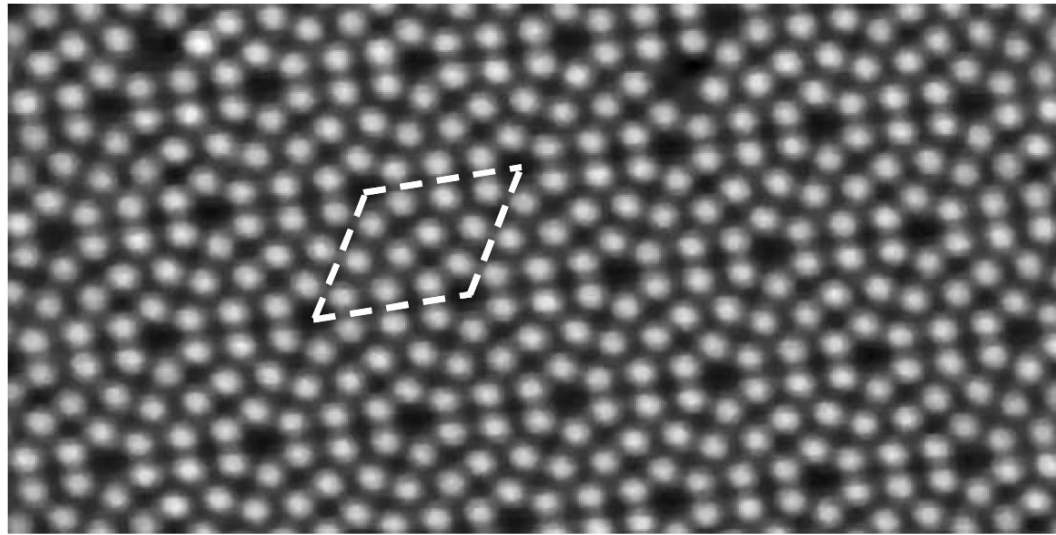


**Fig. 1.21.** STM-image of a Si(111)(7×7) surface. Dashed lines mark the unit cell. The image shows twelve bright spots and one deep and wide hole per unit cell. The bright spots correspond to silicon adatoms bonding to three dangling surface bonds.

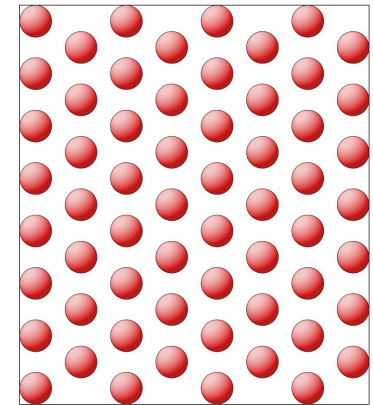
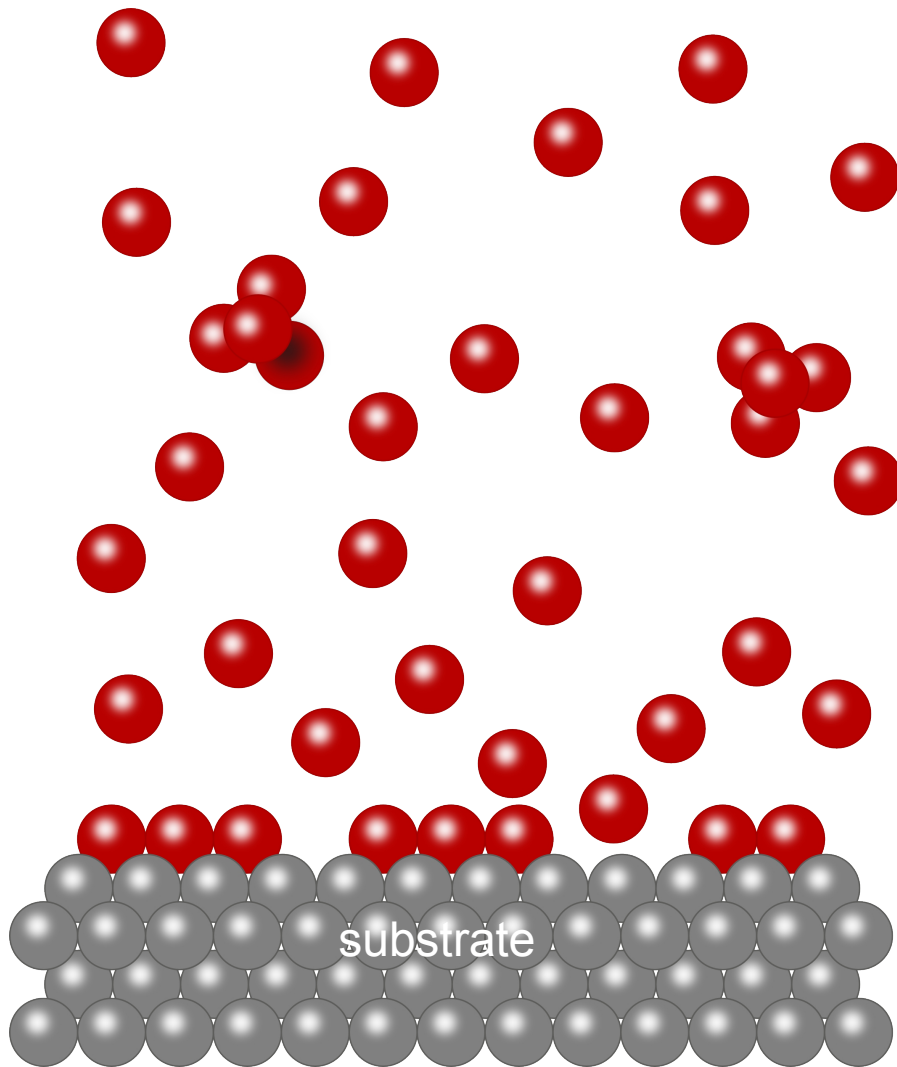


image from [6]: H. Ibach, Physics of Surfaces and Interfaces, Springer-Verlag Berlin Heidelberg 2006

*“Many materials, notably metals, have a surface lattice, which corresponds to the bulk crystallographic (hkl) plane. Merely the atomic distances vertical to the surface plane are changed to a larger or lesser degree, depending on the material, the surface orientation, and the type of bonding.”- H. Ibach [6].*

\*additional atoms (originating for example from steps) are necessary for (7x7) reconstruction to appear [6].

# Introduction



Note the fundamental difference between nucleation within the vapor\* or from melt/solution and the deposition on the substrate:

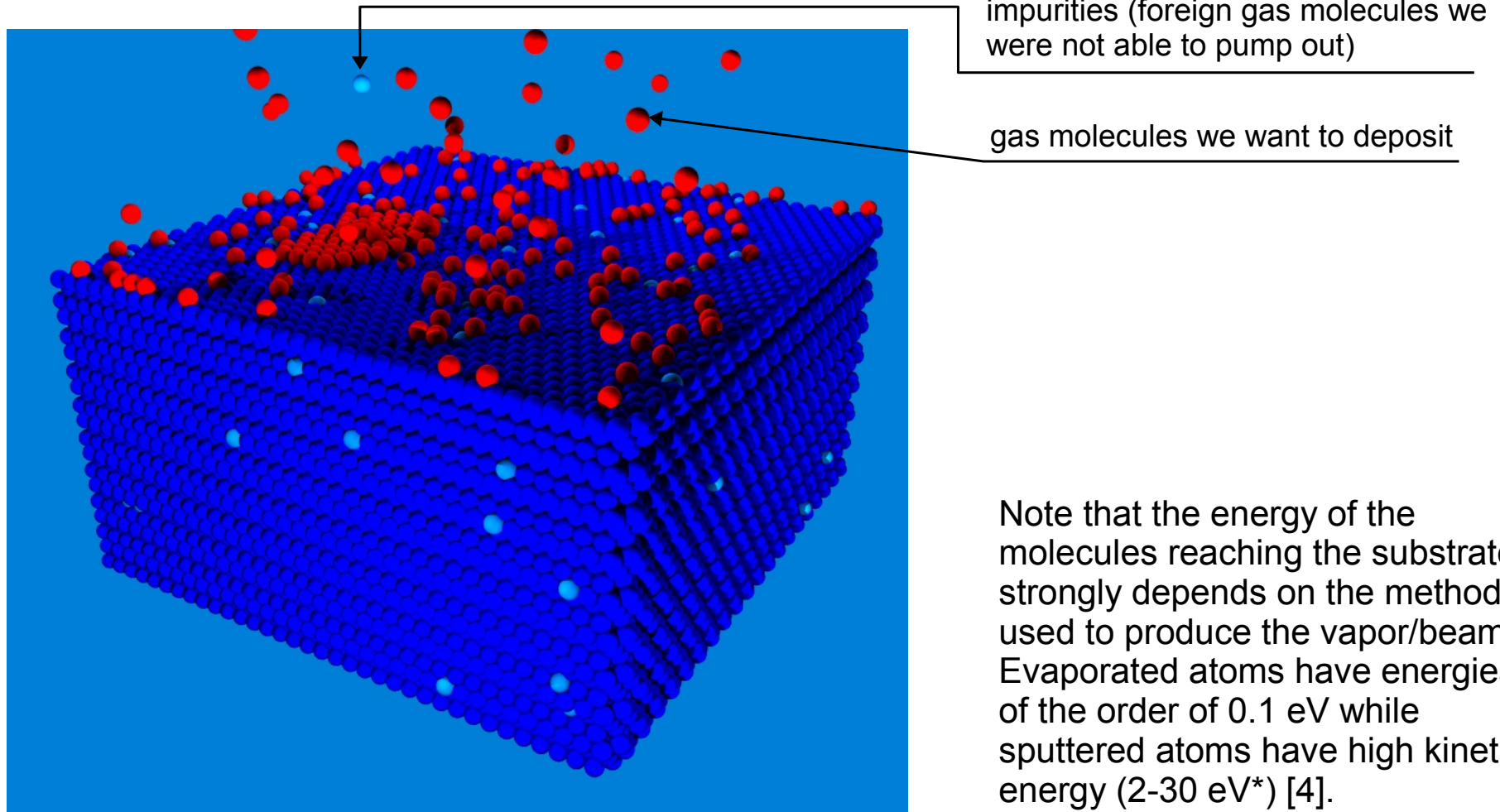
- in the first case the structure of agglomerates (crystalline or amorphous) is influenced by temperature, pressure, vapor composition etc. and depends on a creation of a nucleus (*"Nucleation is the process of random generation of such nanoscopically small formations of the new phase that have the ability for irreversible growth to macroscopically large sizes."* - D. Kashchiev [39])
- in the case of the deposition the nucleus is already present as a substrate

\*see for example *Gas Phase Nanoparticle Formation* entry in Ref. 40.

# Introduction

In previous lecture we have learned how to produce vapors/beams of the molecules to be deposited (evaporation, sputtering etc.)

Now we are interested in the processes taking place when the molecules collide with the substrate.



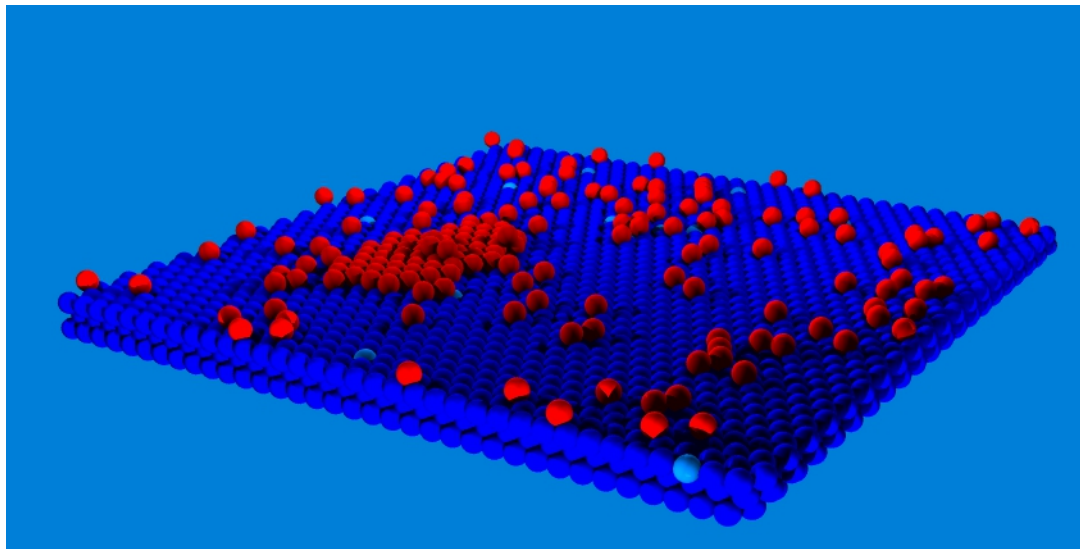
Note that the energy of the molecules reaching the substrate strongly depends on the method used to produce the vapor/beam. Evaporated atoms have energies of the order of 0.1 eV while sputtered atoms have high kinetic energy (2-30 eV\*) [4].

\*depending on acceleration voltage – note that the dependence of energy of atoms is a nonlinear function of accelerating voltage [5].

# Introduction

In previous lecture we have learned how to produce vapors/beams of the molecules to be deposited (evaporation, sputtering etc.)

Now we are interested in the processes taking place when this molecules collide with the substrate.

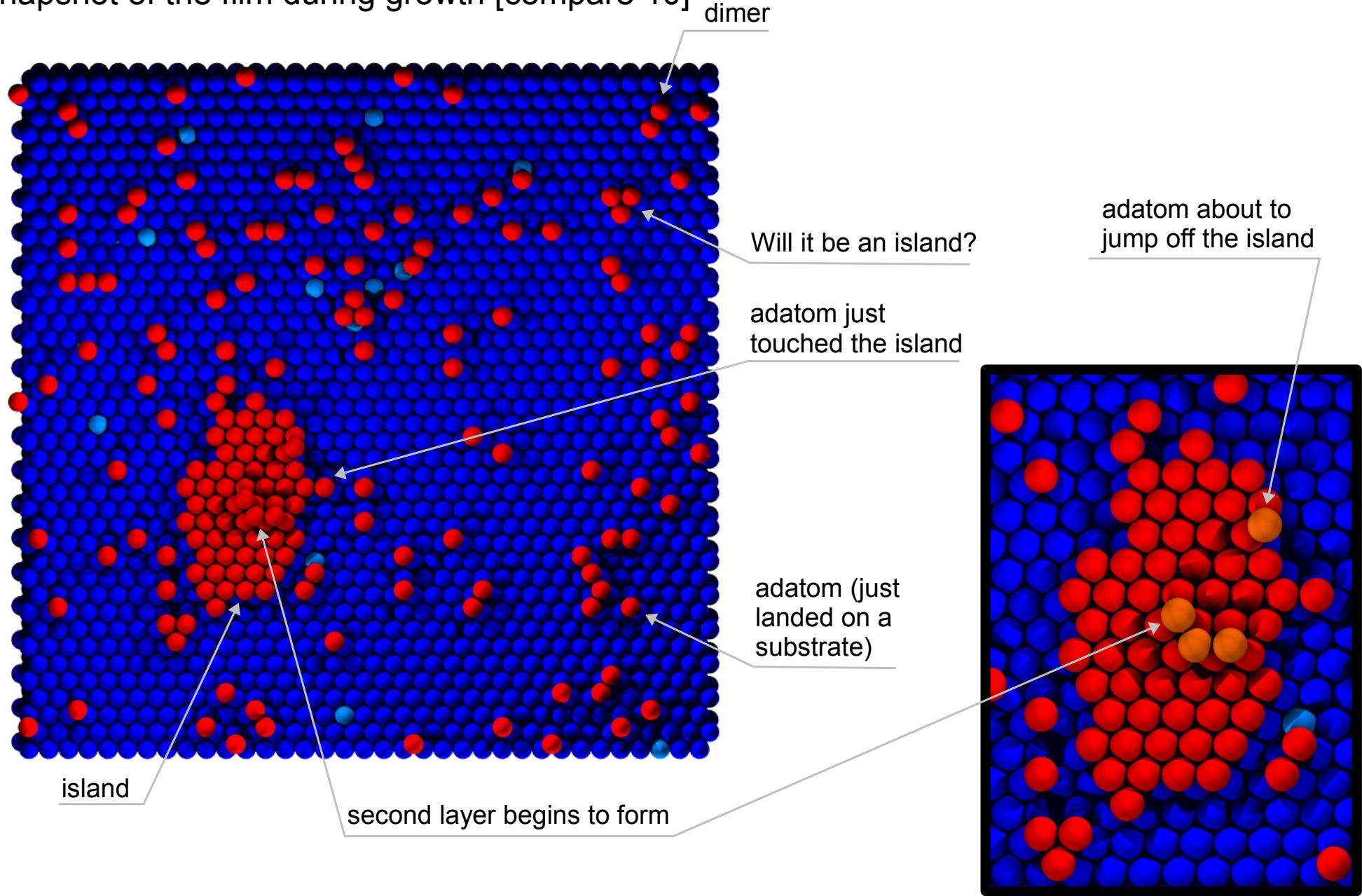


- We make no big error assuming that only near surface atoms of the substrate influence the deposition of molecules\*.
- The deeper layers can play a role in processes like charge out-flow if charged molecules are deposited.

\*the substrate influences the structure of the layers that grow on it but the potential acting on gas molecules is determined by the surface

# Initial growth

Snapshot of the film during growth [compare 10]





# Initial growth

## Potential energy versus coordination number [35]

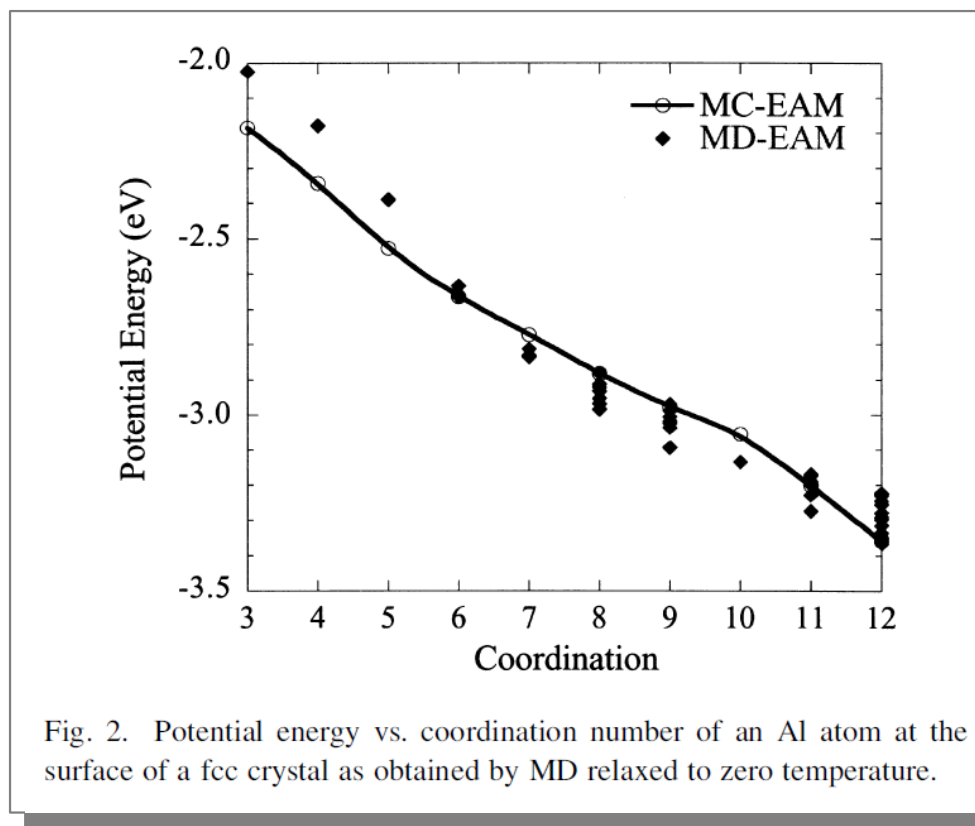
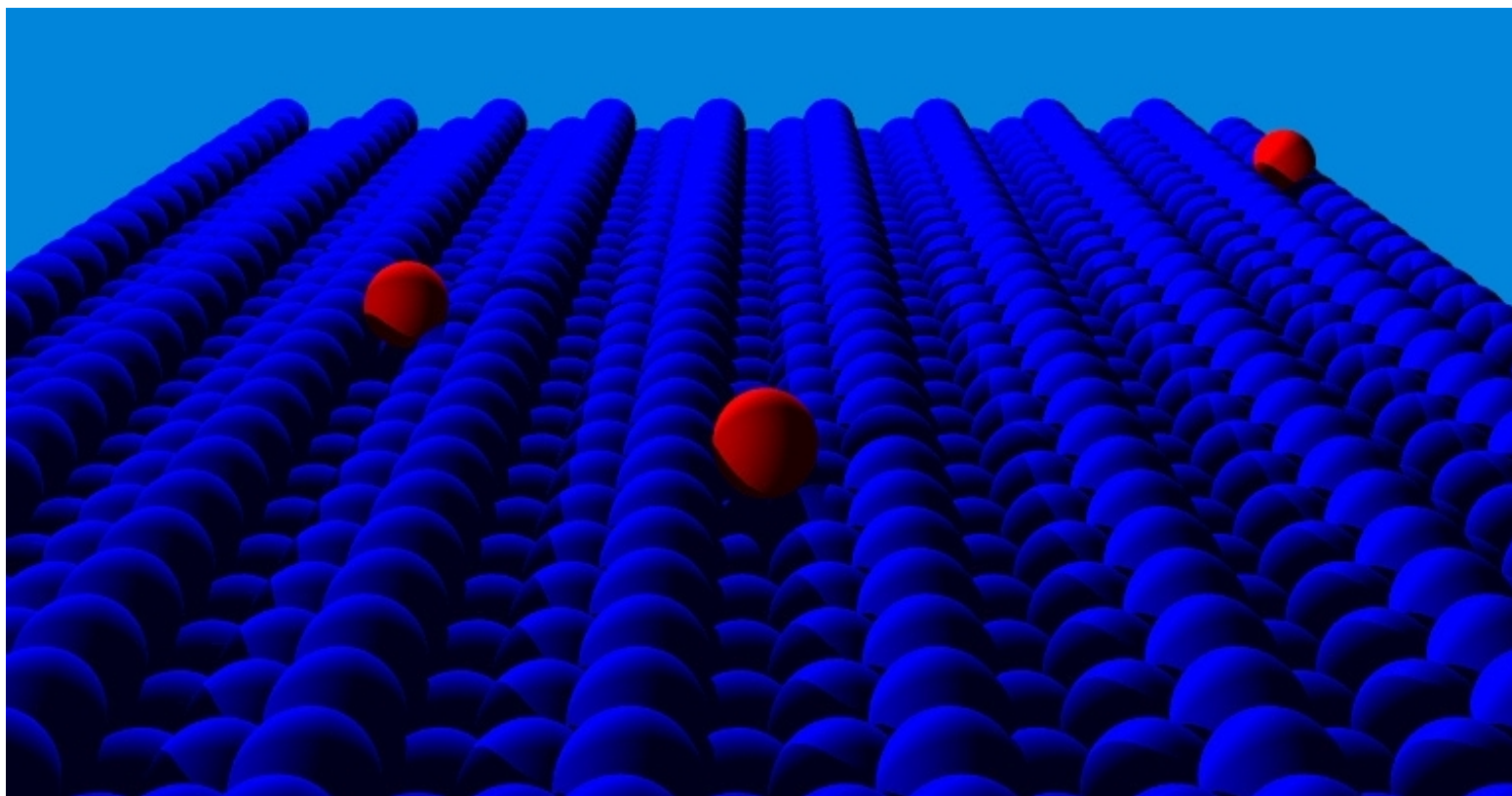


Fig. 2. Potential energy vs. coordination number of an Al atom at the surface of a fcc crystal as obtained by MD relaxed to zero temperature.

*“Atoms of a given coordination number may correspond to surface sites involving different numbers of second neighbors and different types of surface relaxation, and therefore they may have different energies. The diamonds in Fig. 2 are data from several such sites for each coordination number, and it can be seen that they have roughly the same energy.” G.H. Gilmer et al. [35]*

# Initial growth

- Adatoms after touching down on a substrate gradually lose kinetic energy while diffusing on the surface.
- Traditionally it was believed that atoms landing on the substrate carry on random walk until reaching equilibrium position [7].
- In fact the motion is much more complicated and depends on the kind of surface (cut).



- On some channeled surfaces adatom which is moving along the channel performs strictly one-dimensional diffusion [7].

# Initial growth

- On some channeled surfaces adatom which is moving along the channel performs strictly one-dimensional diffusion [7].

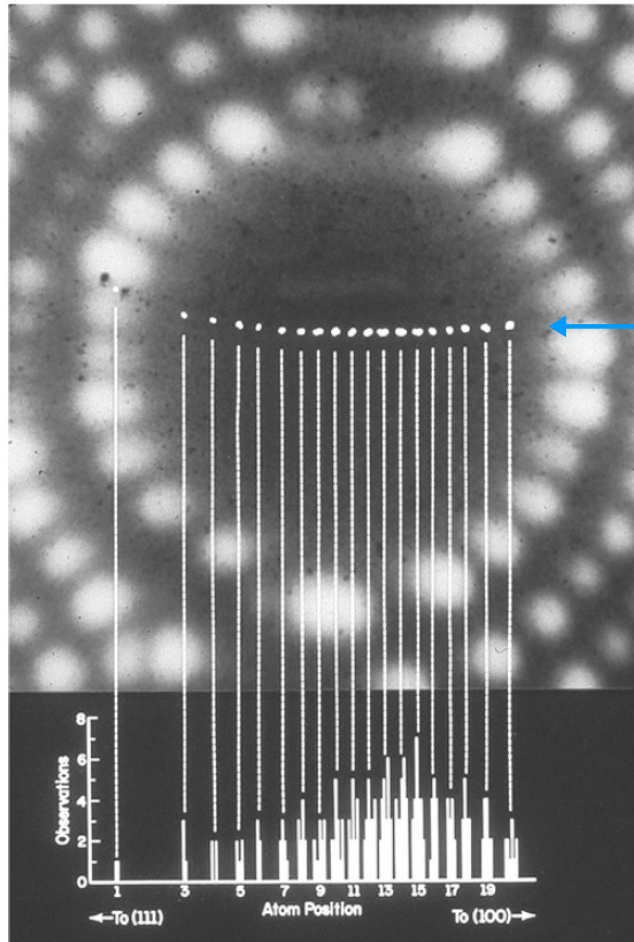


Fig. 4. Location of sites on W(211) at which Rh adatom has been detected after diffusion at 197 K. Motion is strictly one-dimensional. Shown at the bottom is a count of the number sighted at each site.

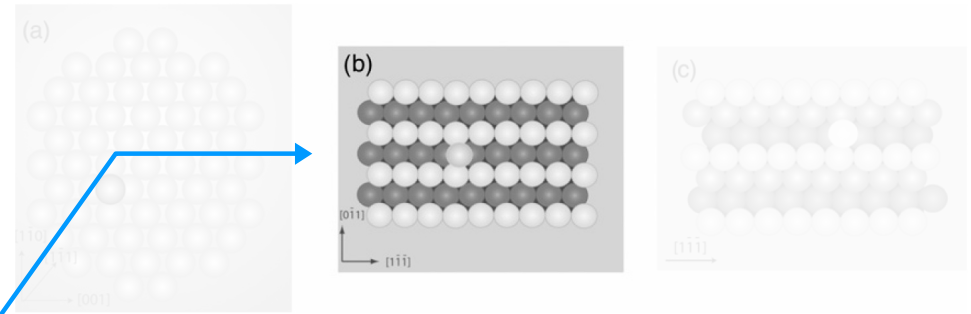


Fig. 1. Hard-sphere models of bcc (a) (110), (b) (211), and (c) (321) planes.

## One-dimensional diffusion of Rh adatom on W(211) surface

graphics from:  
G. Antczak, G. Ehrlich, Surface Science Reports 62, 39 (2007)

# Initial growth

## Cross-channel diffusion

Adatom flux  $J$  can be described by a diffusion equation (one-dimensional form) [7,8]

$$J = -D \frac{\partial c}{\partial x}$$

$D$  - diffusion coefficient

$c$  - adatoms concentration

Often the diffusion coefficient depends on temperature in a usual Arrhenius form [7]:

$$D = D_0 \exp \left[ -\frac{E_d}{k_B T} \right]$$

$E_d$  - activation energy

In practice, due to the difficulties of measuring adatoms flux, the coefficient of diffusion is determined by observing the spread of atoms as a function of time and using Einstein relation giving mean-square displacement [7]:

$$\langle \Delta x^2 \rangle = 2Dt$$

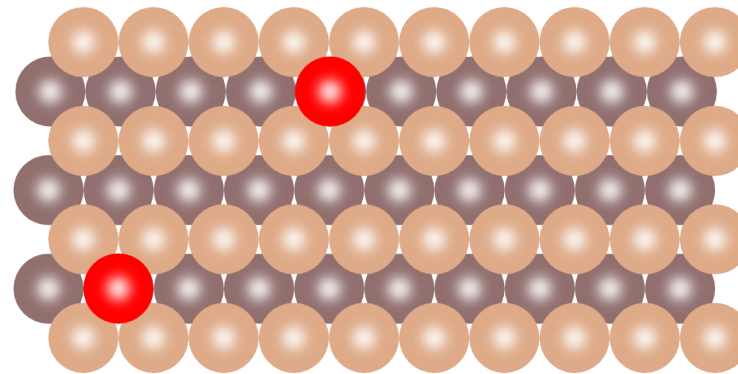
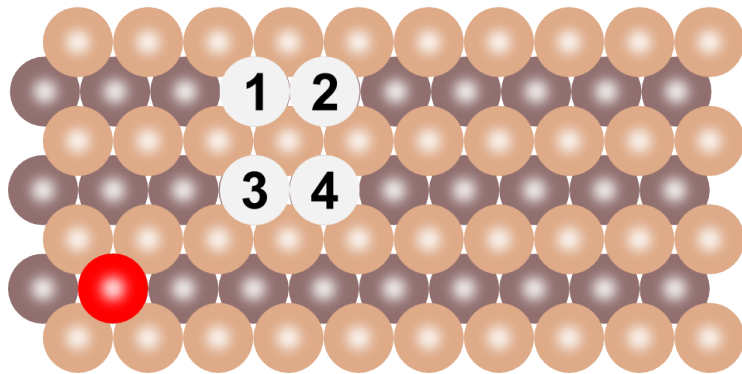
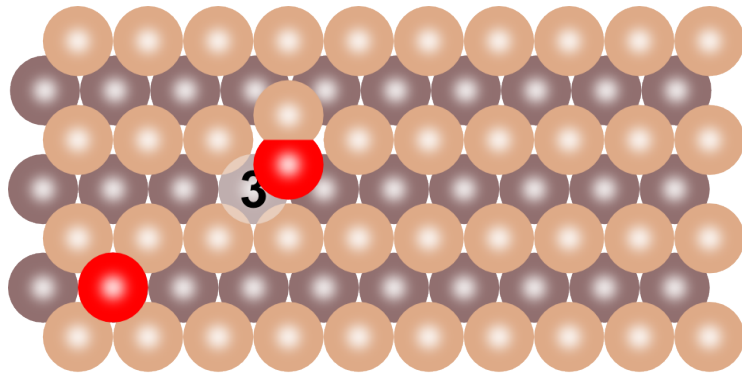
It turns out that on some channeled surfaces the activation energy for the diffusion along the channel is higher than for cross channel diffusion [7].

back  to slide 53

# Initial growth

## Cross-channel diffusion

1. Adatom is located at equilibrium position at site 3.
2. Adatom and one of substrate atoms pair to form a dumbbell which sits at the saddle point.
3. One of the atoms in pair (the atoms are indiscernible) can move to one of four equivalent equilibrium positions (1-4) while other moves to a site in the row of substrate atoms.
4. If the first atom moves to site 1 or 2 the cross-channel diffusion takes place.



# Initial growth

In some cases you may encounter “adclusters” instead of adatoms

- ordered  $\text{Cu}_{147}$  icosahedral\* lands on a  $\text{Cu}(111)$  surface (simulation!)
- velocities up to 4 km/s
- various outcomes: implantation, indentation, disordering, and spreading

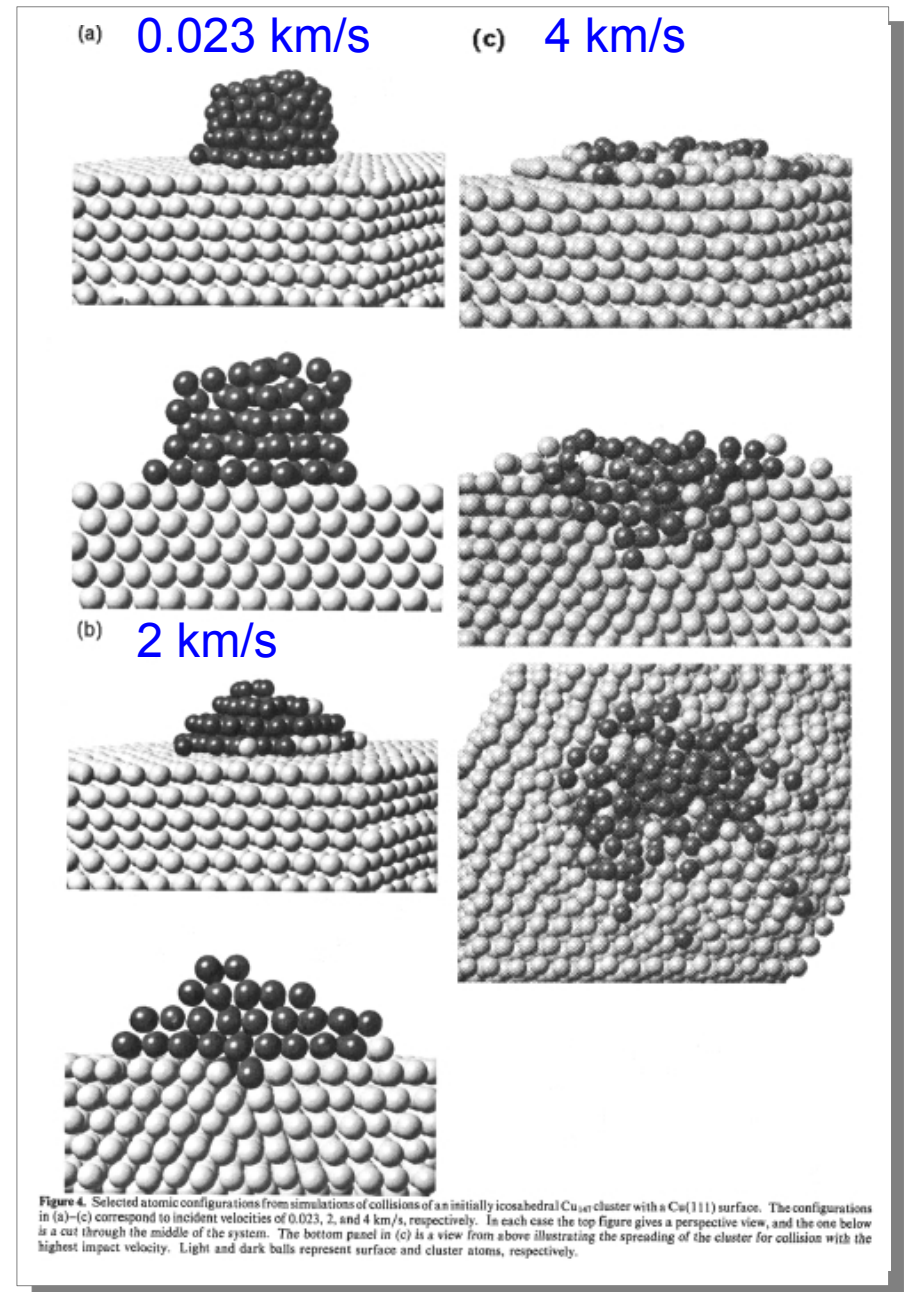


image from: H-P Cheng , U. Landman, J. Phys. Chem. **98**, 3527 (1994)

\*"In geometry, an icosahedron is a polyhedron with 20 triangular faces, 30 edges and 12 vertices." [1]

# Initial growth

**Epitaxy** – *the growth process of a solid film on a crystalline substrate in which the atoms of the growing film mimic the arrangement of the atoms of the substrate* [14].

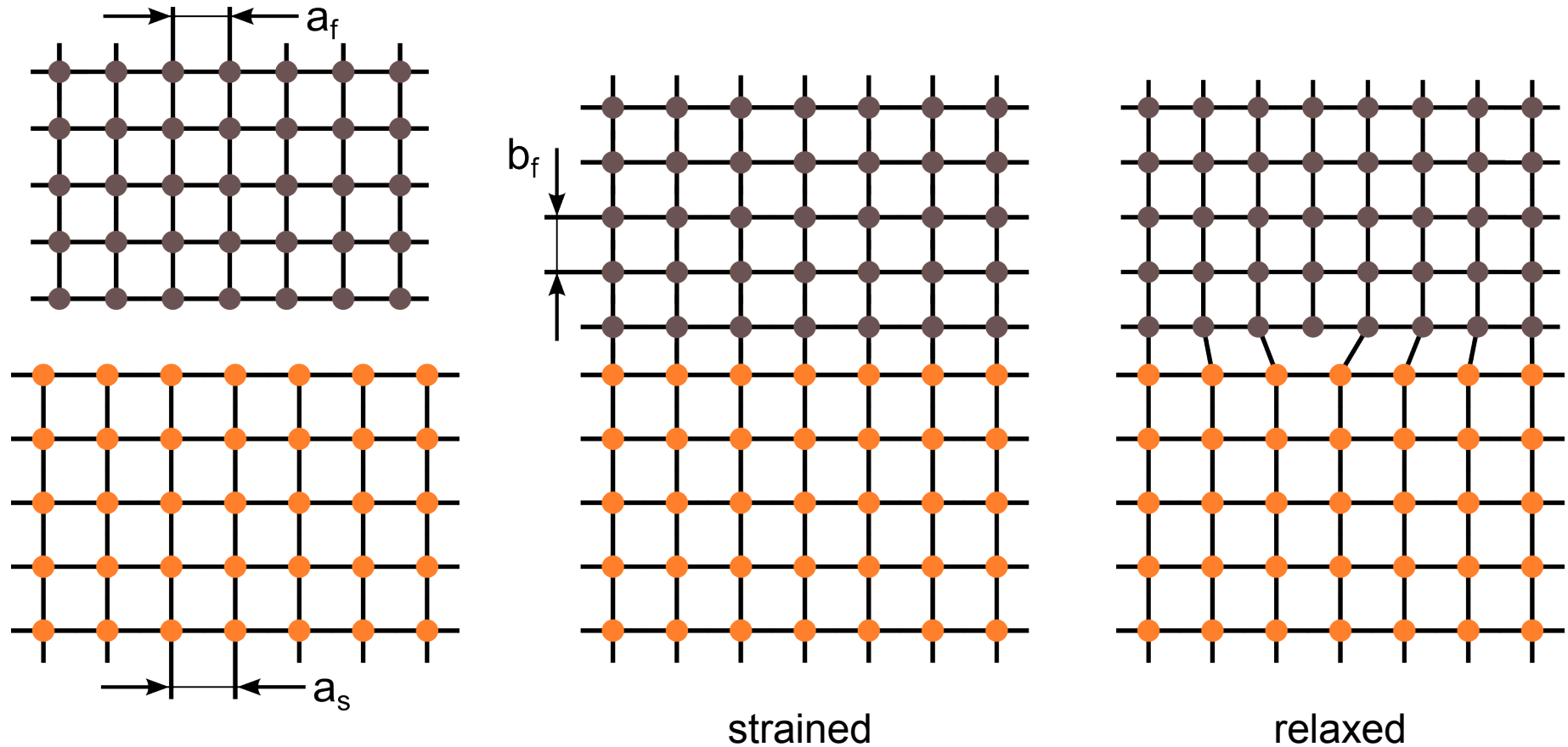
**Homoepitaxy** – growth in a single-component system (eg. Ag on Ag) (substrate and deposits are of the same chemical composition) even if the deposits differs from substrate in dopant concentration (with electrically active impurities → semiconductors).

**Heteroepitaxy** – substrate and deposit have different composition and/or structure

- Epitaxy can be realized with a range of deposition techniques (evaporation, sputtering, chemical vapor deposition etc.)
- The crystalline quality of the deposited films depends however on the technique used (and process parameters, type and purity of the substrate etc.)
- In general lower energies of impinging atoms allow us to obtain better quality films

# Initial growth

**Heteroepitaxy** – substrate and deposit have different composition and/or structure



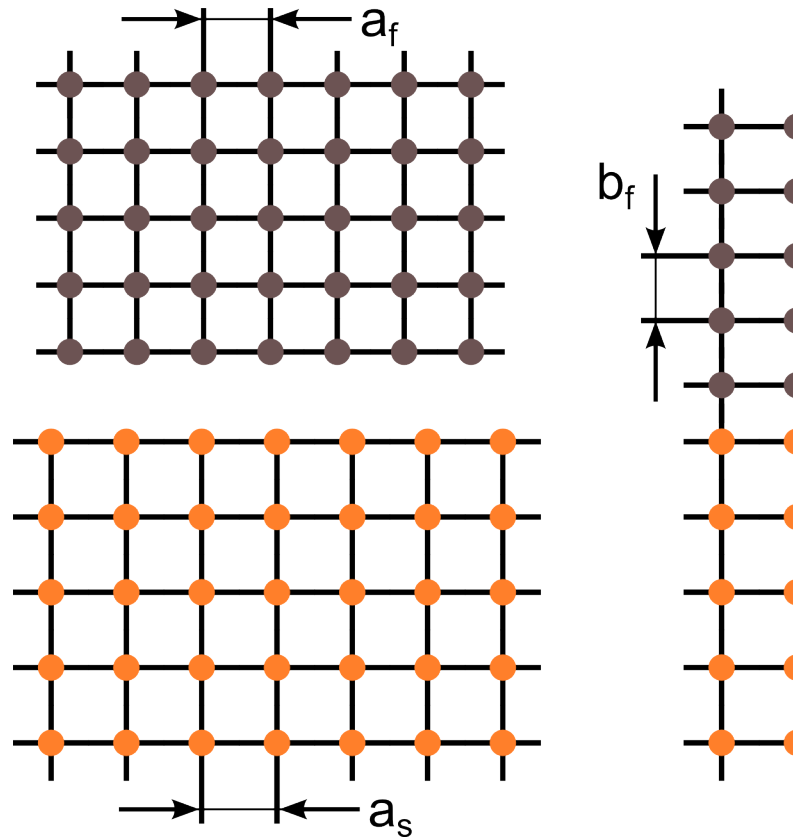
*“In the misfit configuration, the bulk of both layers remains strain free, and the lattice mismatch is accommodated by distortions near the interface and by periodic arrays of incompletely bonded atom rows known as misfit dislocations.” J.C. Bean [32]*

- if the lattice mismatch is not too high the lattice of the epilayer is deformed to become commensurate with the substrate
- the substrate lattice deforms too
- change of  $a_f$  is accompanied by a change of  $b_f$

- if the lattice mismatch is more significant edge dislocation defects form
- *“relaxed epitaxy generally prevails during later film formation stages irrespective of crystal structure or lattice parameters differences” [4]*

# Initial growth

**Heteroepitaxy** – substrate and deposit have different composition and/or structure



Lattice misfit is defined as

$$f = \frac{a_s - a_f}{a_f}$$

To describe epitaxy it is necessary to give the indices of the interface planes and the in plane directions of substrate and film structure which are parallel:

(110)Fe || (110)GaAs; [200]Fe || [100]GaAs

Strained growth can be realized if  $|f| < 0.1$

In certain systems (eg.  $\text{Ge}_x\text{Si}_{1-x}$  on Si) strained (not-relaxed!) epilayers can reach thickness of 1000 nm [4]

# Initial growth

**Heteroepitaxy** – substrate and deposit have different composition and/or structure

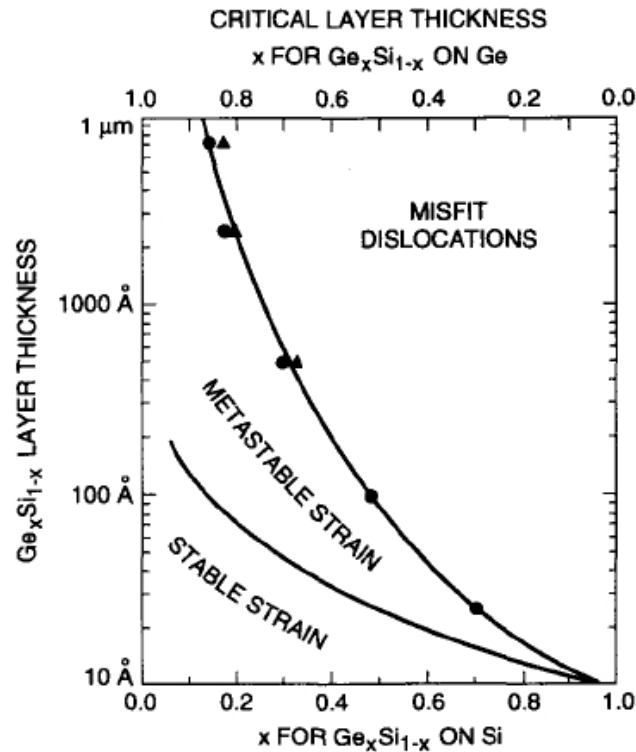


**Fig. 6.** Limits of strained layer (defect-free) growth for  $\text{Ge}_x\text{Si}_{1-x}/\text{Si}$  on (100) Si. Top Right: those thicknesses for which layer thickness and/or Ge fraction is too large to be accommodated purely by strain and misfit dislocations form. Center: configurations in which strained layer growth can be produced at low temperatures but for which strain is metastable and relaxation may ultimately occur upon extended thermal processing. Bottom Left: configurations for which strained layer growth is the lowest energy state and for which dislocations will not form. Upper limit of this equilibrium domain is based on calculations which differ slightly based on underlying assumptions.

Germanium has atomic spacings larger by 4.2% than Si

Metastable strained structure is so stable that it can be processed at temperatures of up to 1000°C [32]

Si substrate lattice is much stiffer, and thicker, than Ge; it remains essentially undistorted

In certain systems (eg.  $\text{Ge}_x\text{Si}_{1-x}$  on Si) strained (not-relaxed!) epilayers can reach thickness of 1000 nm [4]

image from: J.C. Bean, Proceedings of the IEEE **80**, 571 (1992)

# Initial growth

**Heteroepitaxy** – substrate and deposit have different composition and/or structure

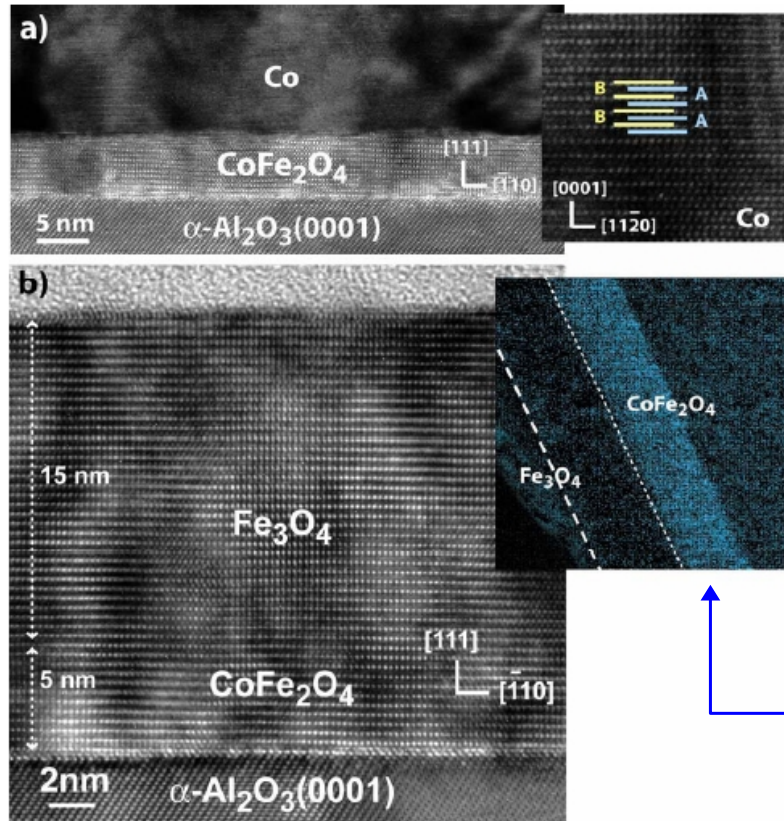


FIG. 3. (Color online) Cross-sectional HRTEM images of (a)  $\text{CoFe}_2\text{O}_4(5\text{ nm})/\text{Co}(15\text{ nm})$  and (b)  $\text{CoFe}_2\text{O}_4(5\text{ nm})/\text{Fe}_3\text{O}_4(15\text{ nm})$  bilayers viewed along the  $[11\bar{2}]$  zone axis. The right inset of (a) represents a zoom of the  $\text{Co}(0002)$  planes viewed along  $[\bar{1}10]$ . The EELS chemical map of the Co concentration in another  $\text{CoFe}_2\text{O}_4(15\text{ nm})/\text{Fe}_3\text{O}_4(15\text{ nm})$  bilayer is shown in the inset of (b).

- deposited with oxygen-assisted MBE (base pressure  $10^{-9}$  Pa)
- perfect structure of the bilayer
- abrupt interfaces
- high homogeneity
- very low deposition speed ( $\sim 0.001\text{ nm/s}$ )

no Co in  $\text{Fe}_3\text{O}_4$

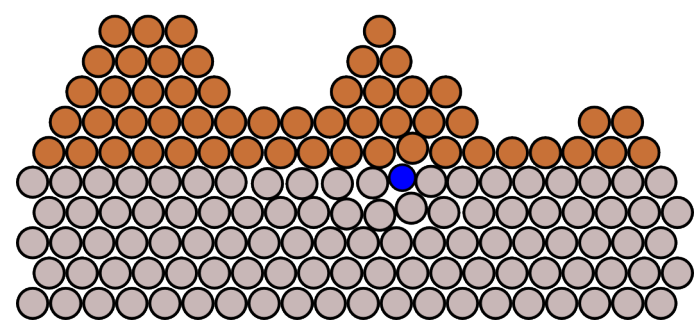
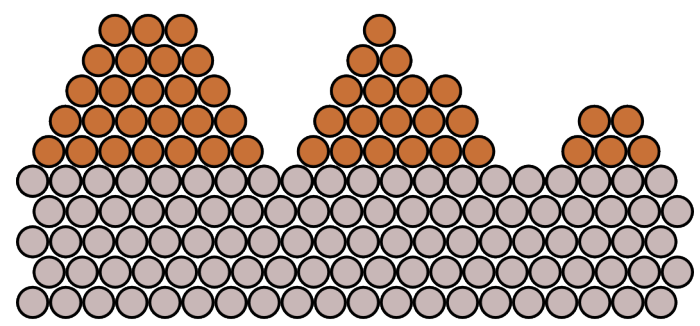
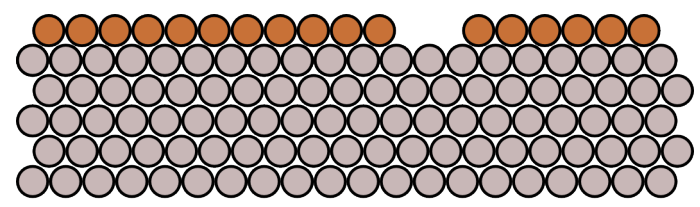
To guarantee the low contamination (say, less than 0.001% of impurities) the deposition time of 1 ML of rest gases in the chamber must be of the order of  $10^5\text{ s}$  which requires a vacuum better than approx.  $10^{-9}$  Pa (the estimate does not include different sticking coefficients and re-evaporation of deposited material) [14]

image from: A.V. Ramos, J.-B. Moussy, M.-J. Guittet, M. Gautier-Soyer, C. Gatel, P. Bayle-Guillemaud, B. Warot-Fonrose, E. Snoeck, Phys. Rev. B **75**, 224421 (2007)

# Initial growth

Basic modes of thin film growth [4]:

- layer (Frank-van der Merwe) – adatoms are more strongly bound to the substrate than to each other (2-D islands)
- island (Volmer-Weber) – happens when adatoms attract each other stronger than they are bound to the substrate (3-D islands)
- Stranski-Krastanov – “*layer plus island*”; after one or more monolayers are formed the island growth becomes more favorable. There can be many physical causes; e.g. the energy released when the lattices at the interface relax\* may contribute to island formation [4]

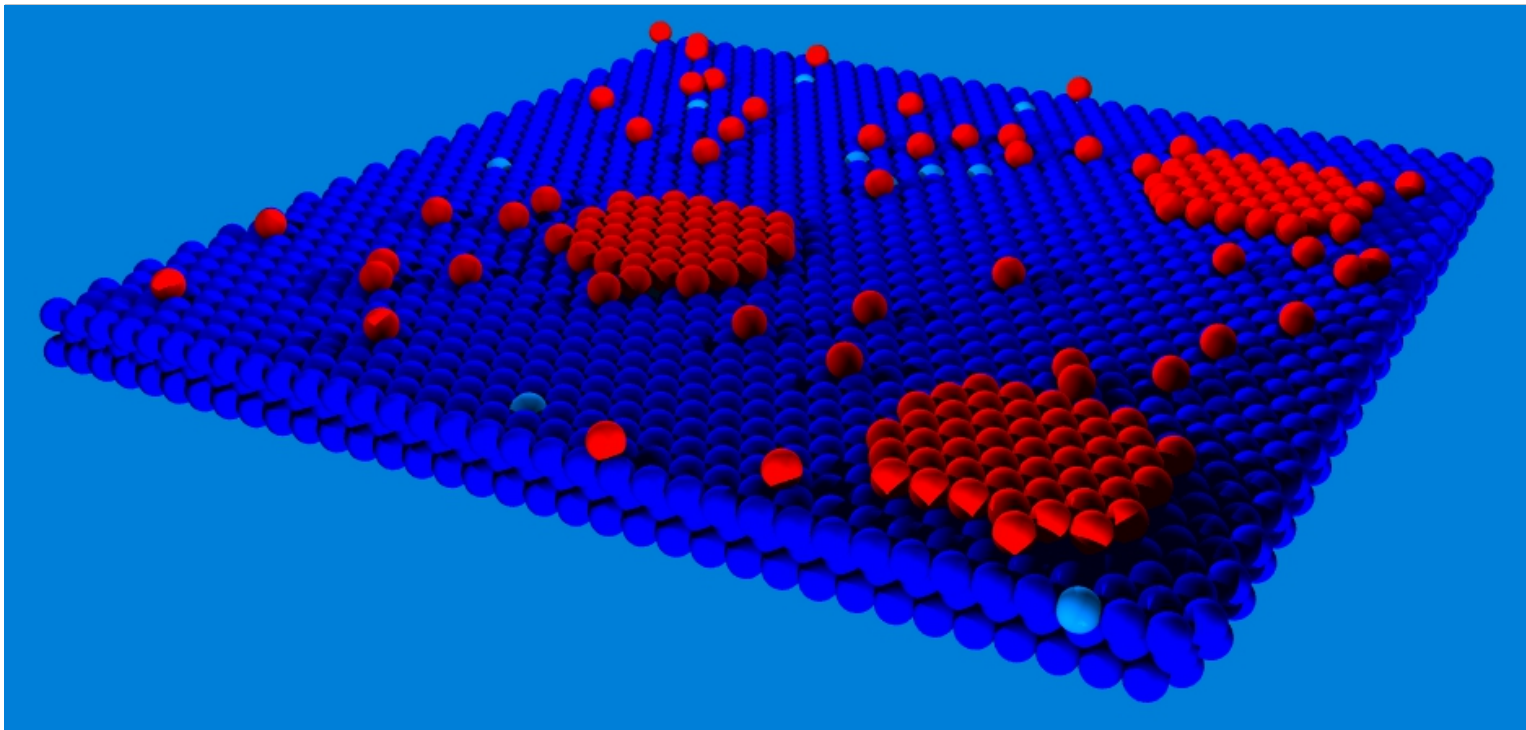
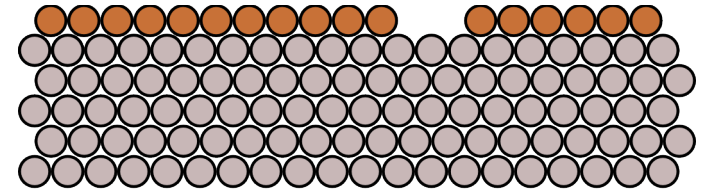


\*there is often a mismatch between bulk lattice parameters of the substrate and the deposit

# Initial growth

Basic modes of thin film growth [4]:

- layer (Frank-van der Merwe) – adatoms are more strongly bound to the substrate than to each other (2-D islands)



Growth of islands incorporates adatoms from the adjacent areas leaving place for further nucleation

# Initial growth

Basic modes of thin film growth [4]:

- layer (Frank-van der Merwe) – adatoms are more strongly bound to the substrate than to each other (2-D islands)

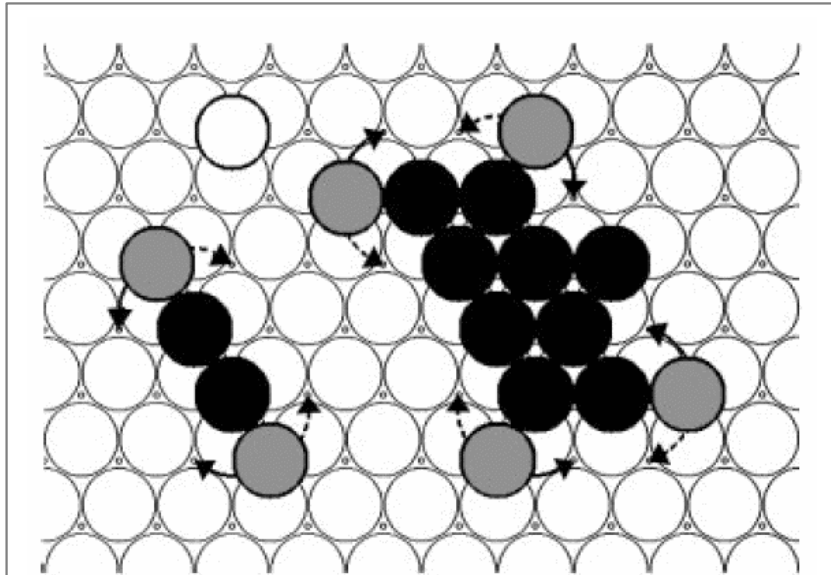


FIG. 3. Ball model of small agglomerates on Pt(111). The lightly shaded atoms are only onefold coordinated in plane. Dashed and full arrows indicate diffusional jumps into twofold coordinated sites via atop positions and via bridge positions, respectively.

Adatoms in the course of diffusion tend to occupy higher coordinated sites (having more neighbors) [9]

figures from:  
 M. Hohage, M. Bott, M. Morgenstern,  
 Z. Zhang, T. Michely, G. Comsa  
 Phys. Rev. Lett. **76**, 2366 (1996)

Increased temperature favors increased number of neighbors – due to easier diffusion:

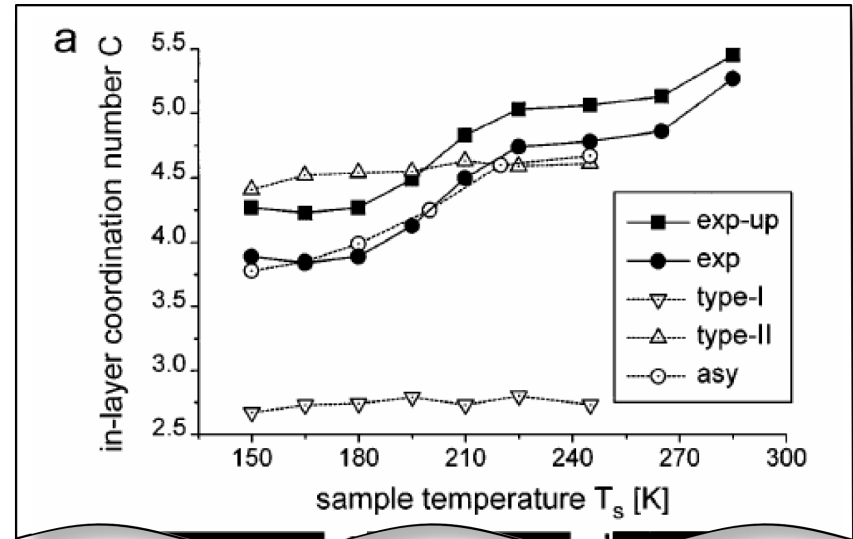


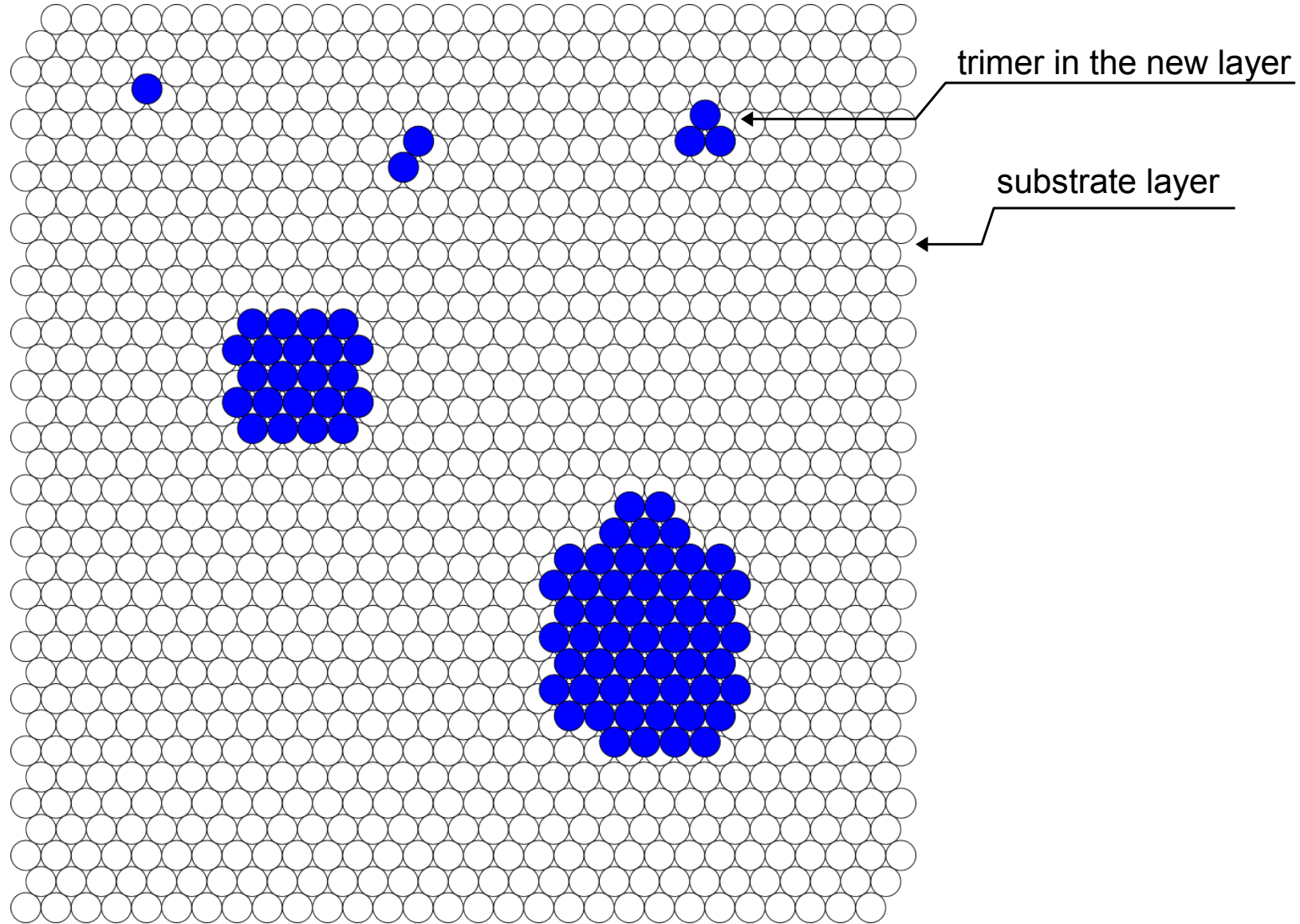
figure cut here

FIG. 2. (a) Temperature dependence of average in-plane coordination number  $C$  of atoms in Pt dendrites. Full symbols result from transformation of  $d_{true}$  under the assumption of atomically smooth branches (exp-up) and of every fifth edge atom contributing to branch roughness (exp). Open symbols result from MC simulations assuming hit-and-stick growth (type I), immobile bonding only in twofold coordinated sites (type II), and temperature dependent asymmetry in jump probability from onefold to twofold coordinated sites (asy) (see also text). Simulated island shapes at 180 K of type I (b), type II (c), and with the asymmetry assumption (d).

Increased temperature favors diffusion and layer growth [9] (**simulation!**)

# Initial growth

Island size vs. average coordination number\*

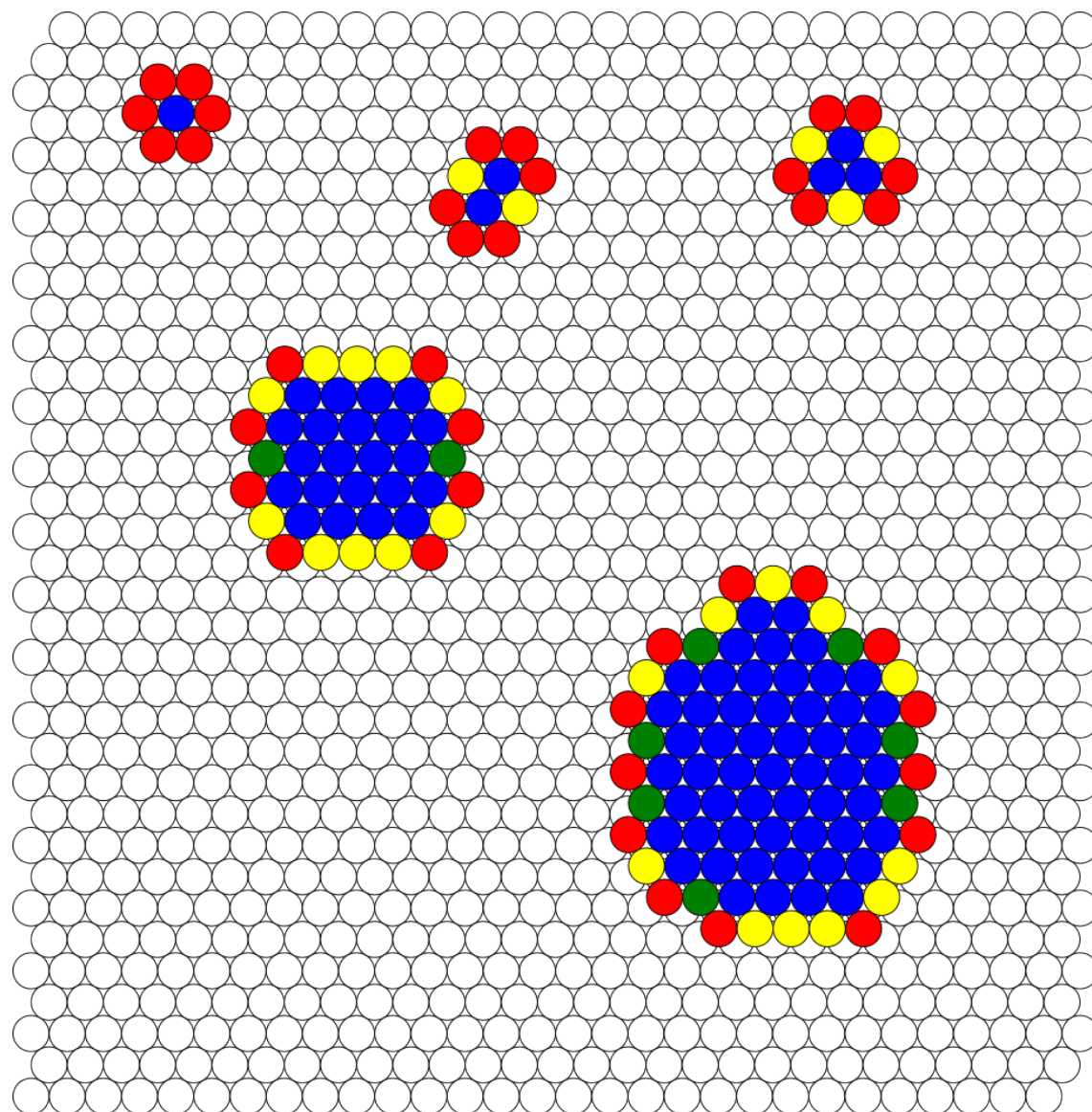


arbitrary positions of islands – not simulated!

\*not counting the bounds with the substrate atoms

# Initial growth

Island size vs. average coordination number



coordination number of a site

- 1
- 2
- 3

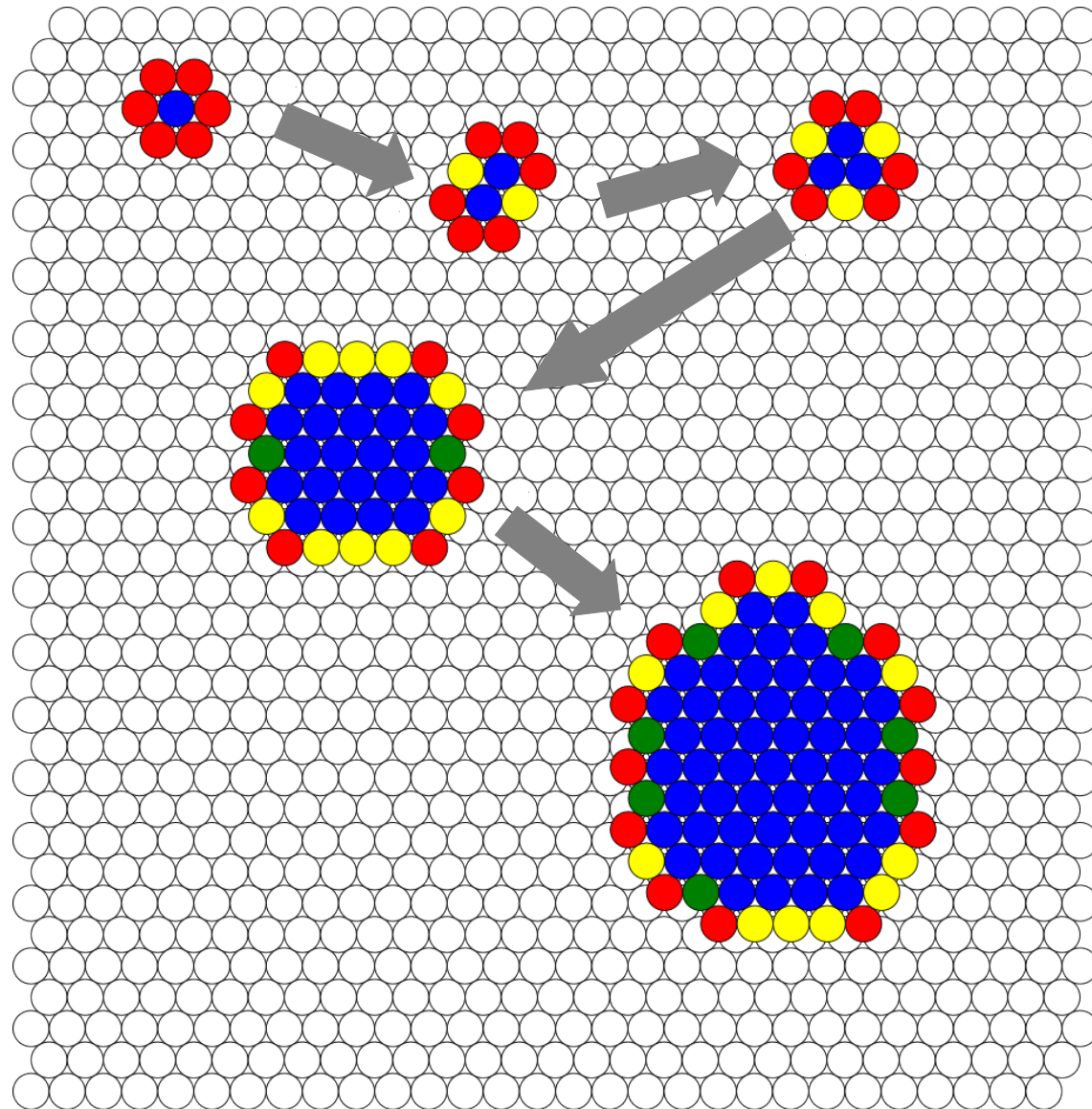
Number of atoms in an island	Average coordination number of sites bordering the island*
1	1
2	1.25
3	1.3(3)...
22	1.7
54	1.806...

arbitrary positions of islands – not simulated!

\*relevant for this picture only

# Initial growth

## Island size vs. average coordination number



arbitrary positions of islands – not simulated!

coordination

number of atoms of a smaller island

- On average a molecule that attaches itself to a bigger island has more neighbors from that island that would be the case for smaller island

- This results, again on average, in higher energy gain (decrease) if the adatom joins bigger island

- There is energy gain too if an atom leaves a smaller island and joins the bigger one

- This is similar to the case of bigger rain drops growing at the cost of smaller ones (the vapor pressure is smaller the smaller droplet radius) [17]

22 1.7

54 1.806...

\*relevant for this picture only

# Initial growth

There is an “infinite number” of island shapes

“notice that two boundary steps of a hexagon, which meet at one corner, are geometrically inequivalent relative to the substrate” [10]

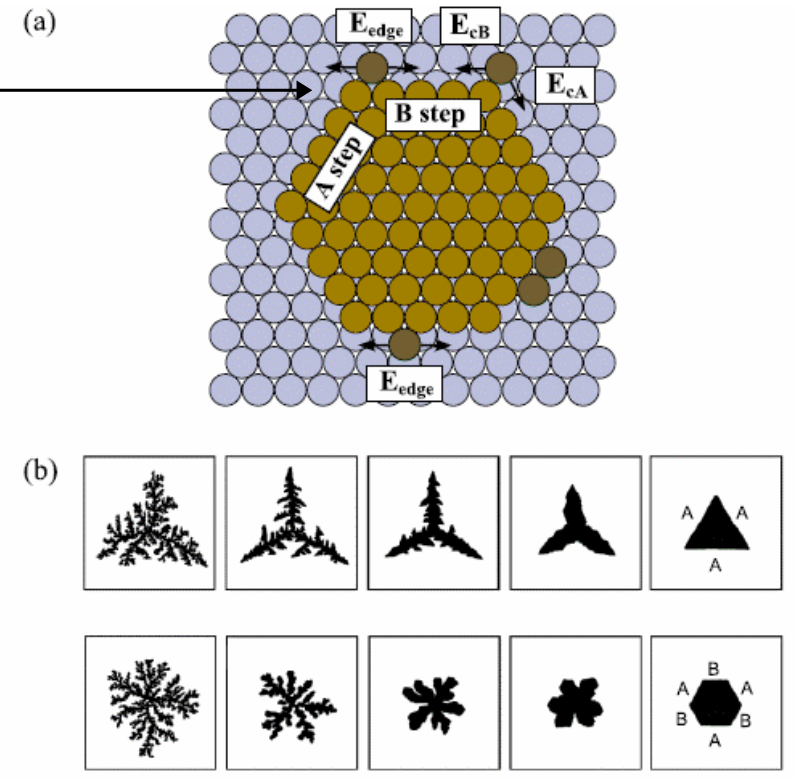
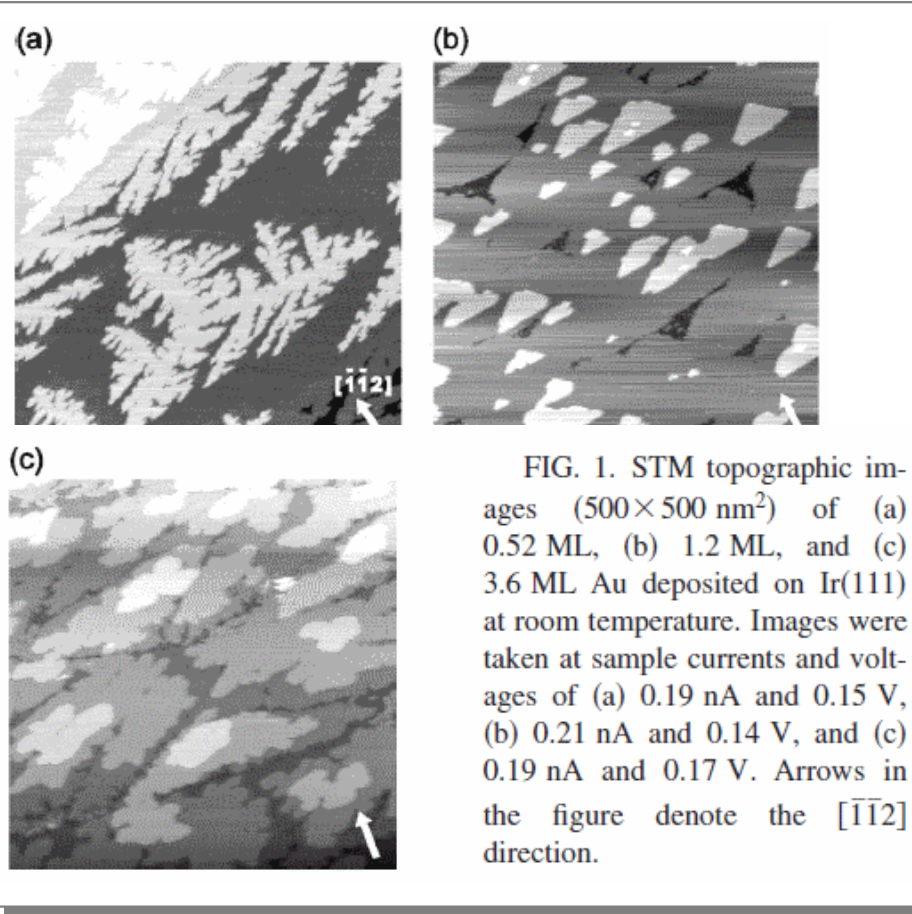


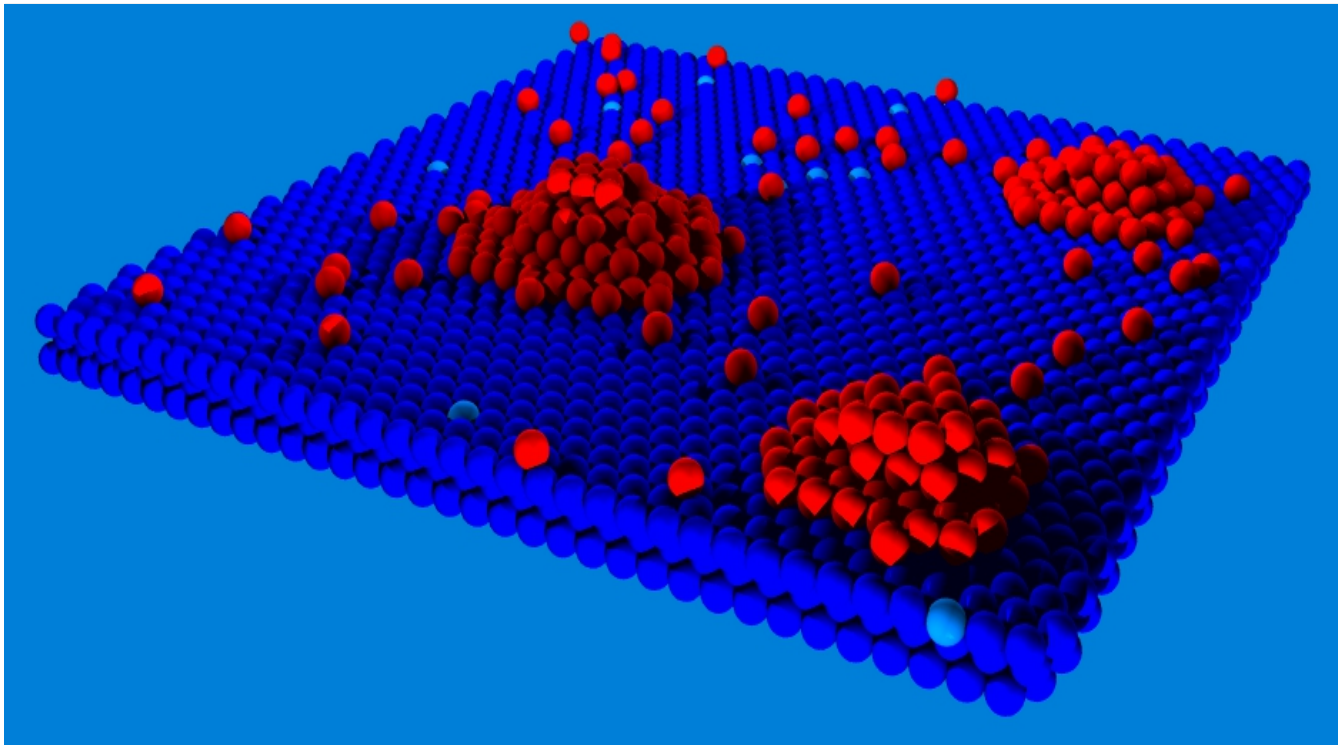
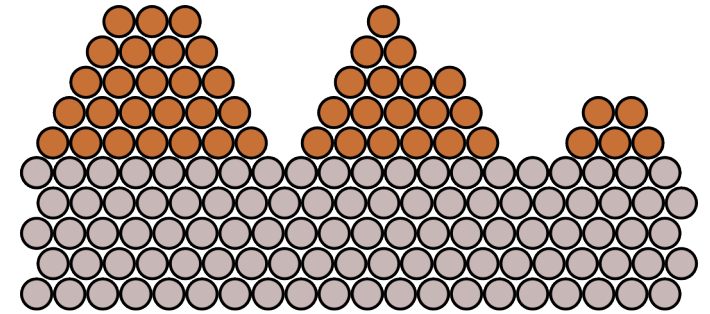
image from: S. Ogura, K. Fukutani, M. Matsumoto, T. Okano, M. Okada, T. Kawamura, Phys. Rev. B **73**, 125442 (2006); rearranged

image from: M. Einax, W. Dieterich, P. Maass, Rev. Mod. Phys. **85**, 921 (2013)

# Initial growth

Basic modes of thin film growth [4]:

- island (Volmer-Weber) – happens when adatoms attract each other stronger than they are bound to the substrate (3-D islands)



Many systems of metals on insulators grow in that mode [4]

# Initial growth

Basic modes of thin film growth [4]:

- island (Volmer-Weber) – happens when adatoms attract each other stronger than they are bound to the substrate (3-D islands)
- “*Self-organization phenomena at semiconducting surfaces allow **fabrication of quantum dot structures for novel nanodevices** with unprecedented applications in optoelectronics, as well as single electron transistors operating at room temperature and/or resonant tunneling structures. Other applications, such as nanocrystal memories, require high-density ultrasmall dots embedded in insulating layers without the need of quantum confinement effects.*” [19]

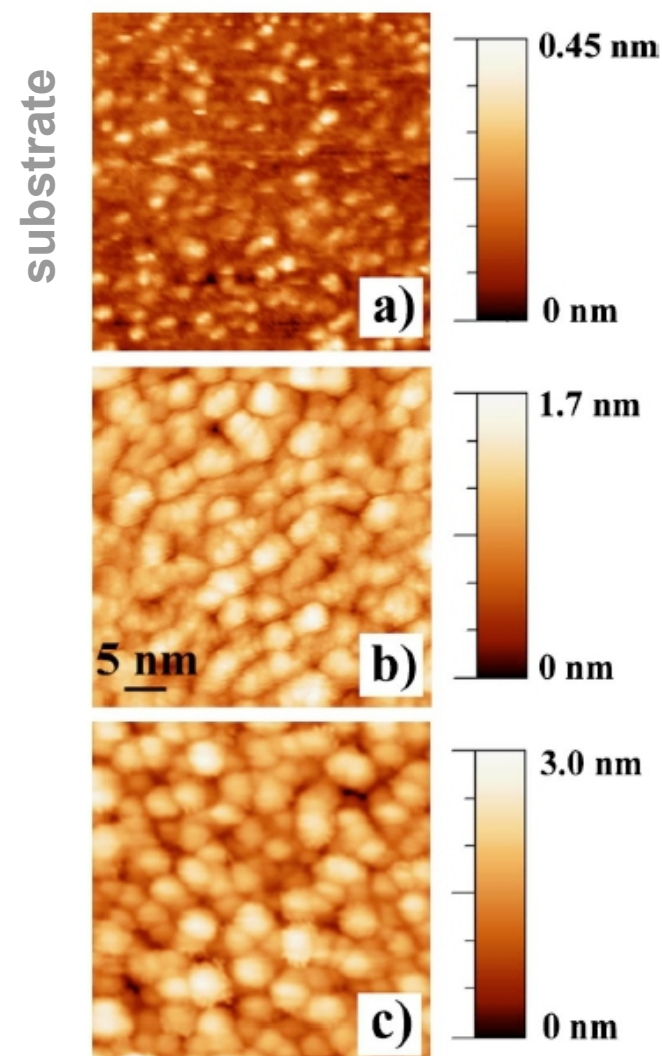


image from: I. Berbezier, A. Karmous, A. Ronda, A. Sgarlata, A. Balzarotti, P. Castrucci, M. Scarselli, M. De Crescenzi, Appl. Phys. Lett. **89**, 063122 (2006)

FIG. 1. (Color online) (a) STM image of the SiO<sub>2</sub> substrate.  $V_{\text{sample}} = -3.0$  V,  $I = 0.5$  nA. (b) STM image of 4 MLs of Ge deposited on SiO<sub>2</sub>/Si(001) surface kept at room temperature.  $V_{\text{sample}} = 2.0$  V,  $I = 1.0$  nA. (c) STM image of the sample shown in panel (b) after annealing at 500 °C for 30 min.  $V_{\text{sample}} = 3.0$  V,  $I = 0.5$  nA. Grayscale ranges (at right) confirm the sizable changes in the rms roughness values passing from the bare SiO<sub>2</sub> substrate to the amorphous Ge film and the Ge dots.

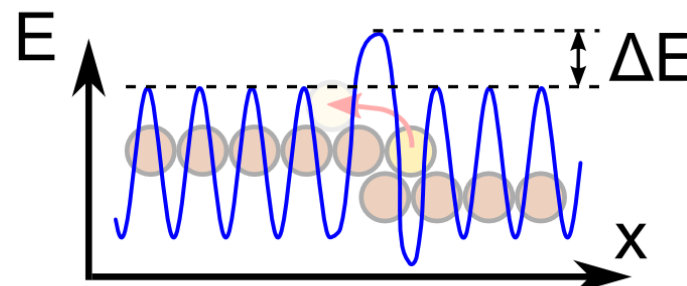
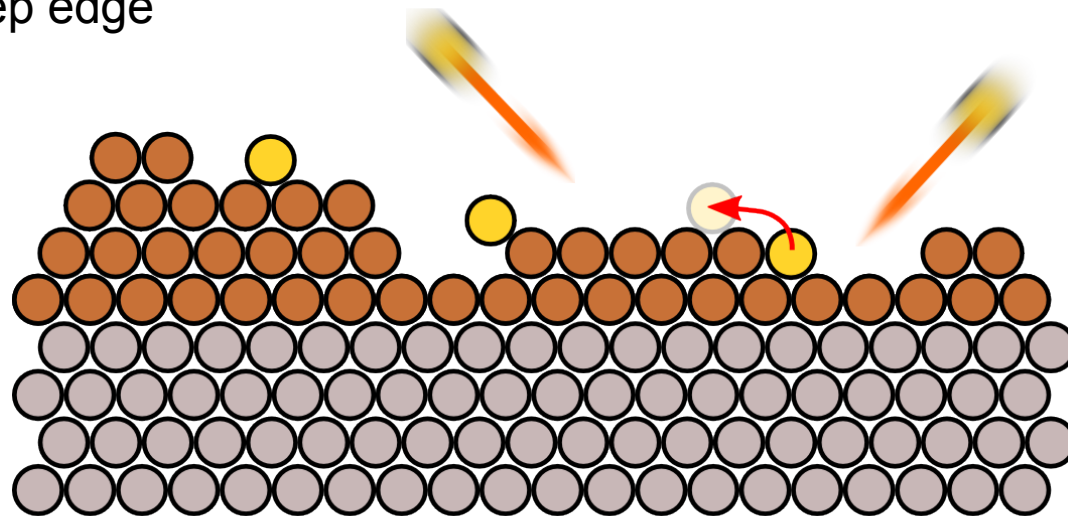
# Initial growth

## Ehrlich-Schwoebel barrier [10,12]

- adatom can be incorporated into the structure of the film in the layer it lands on
- other adatoms diffuse to terraces and can perform interlayer jump requiring some additional energy (Ehrlich-Schwoebel barrier)
- the barrier is associated with low-coordinated site/position (lower number of near neighbors than on flat surface) at a step edge

The values of the barrier depend strongly on the system and orientation of surfaces between which the diffusion takes place\* (3-dimensional barrier) and often determine the evolution of the surface micro-structure [13].

The energy barriers are of the order of tenths of eV [12,13].



\*for example the barrier is different for  $\{111\} \rightarrow \{111\}$  diffusion (different layers on the same face) and  $\{111\} \rightarrow \{100\}$  (faces of an island or grain)

# Initial growth

## Ehrlich-Schwoebel barrier [10,12]

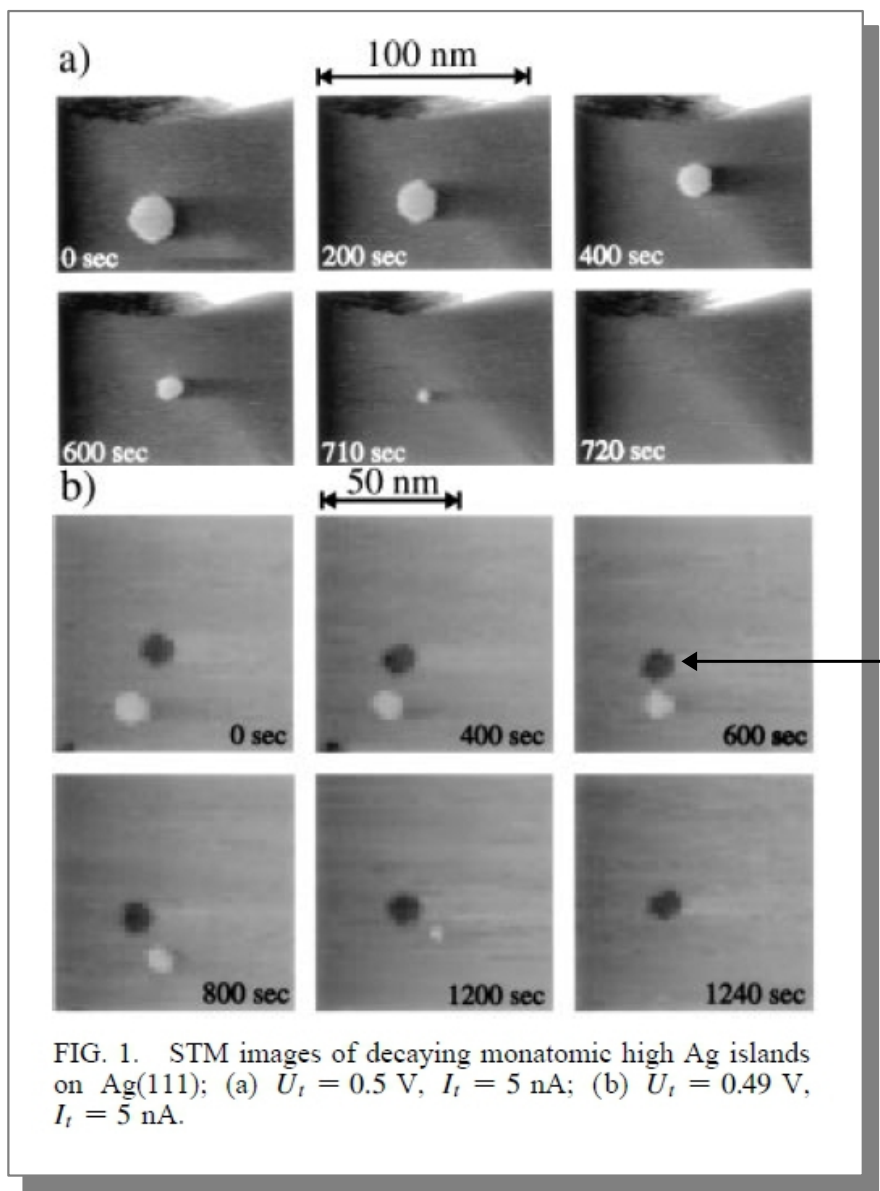


FIG. 1. STM images of decaying monatomic high Ag islands on Ag(111); (a)  $U_t = 0.5$  V,  $I_t = 5$  nA; (b)  $U_t = 0.49$  V,  $I_t = 5$  nA.

RT; Ag on Ag(111)

- the monoatomic Ag island decays as a result of diffusion
- *“Obviously, the adatoms evaporating from the adatom island do not fill the vacancy island: The vacancy island area does not decrease while the adatom island disappears completely. The adatoms detaching from the adatom island prefer to diffuse to some other place which is presumably an ascending step not visible on the image. **This observation provides a direct and independent proof for the existence of a step edge barrier opposing downward diffusion of adatoms across a step.**” [21]*

a monatomic\* deep vacancy island

image from: K. Morgenstern, G. Rosenfeld, G. Comsa, Phys. Rev. Lett **76**, 2113 (1996)

\*monatomic - consisting of one atom ([www.merriam-webster.com](http://www.merriam-webster.com) [28])

# Initial growth

## Ehrlich-Schwoebel barrier [10,12]

RT; Ag on Ag(111)

- the monoatomic Ag island decays as a result of diffusion
- the adatom islands move while decaying
- diffusivity of the islands increases with decreasing island size

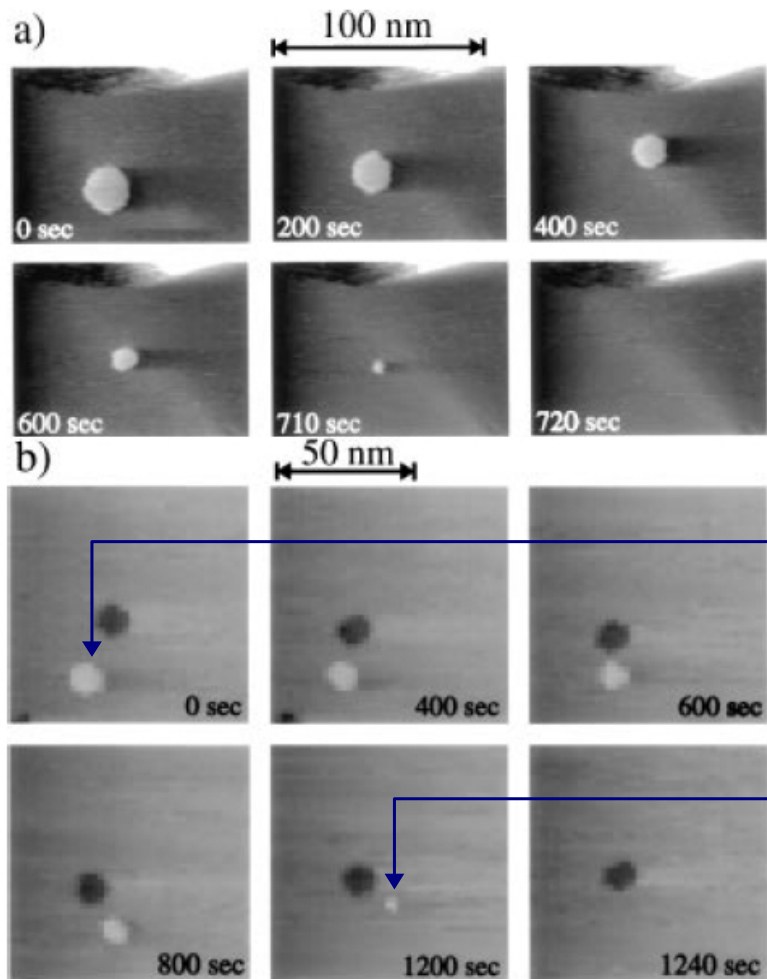


FIG. 1. STM images of decaying monoatomic high Ag islands on Ag(111); (a)  $U_t = 0.5$  V,  $I_t = 5$  nA; (b)  $U_t = 0.49$  V,  $I_t = 5$  nA.

image from: K. Morgenstern, G. Rosenfeld, G. Comsa, Phys. Rev. Lett **76**, 2113 (1996)

\*monoatomic - consisting of one atom ([www.merriam-webster.com](http://www.merriam-webster.com))

# Initial growth

Magic 2-D clusters – certain sizes of islands are more stable

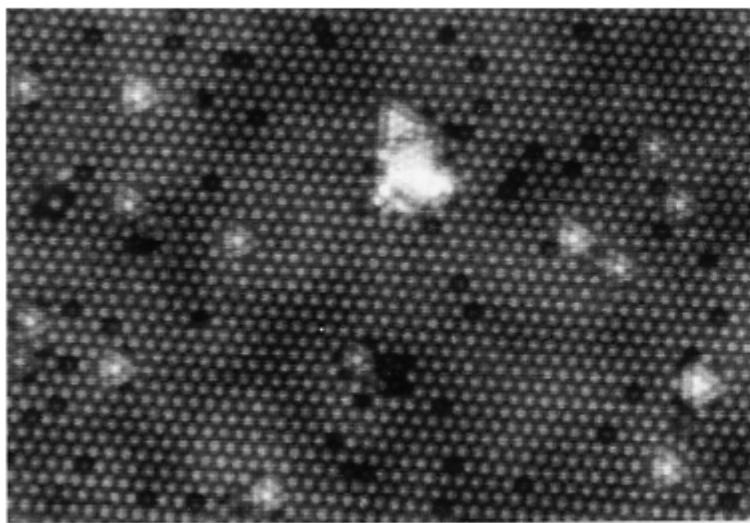


FIG. 1. STM image (size =  $31 \times 21 \text{ nm}^2$ ) of 2D clusters on the  $\sqrt{3} \times \sqrt{3} R30^\circ$  Ga/Si(111) surface. Image was obtained with the tip bias  $V_t = -1.6 \text{ V}$  and tunneling current  $I_t = 1.8 \text{ nA}$ .

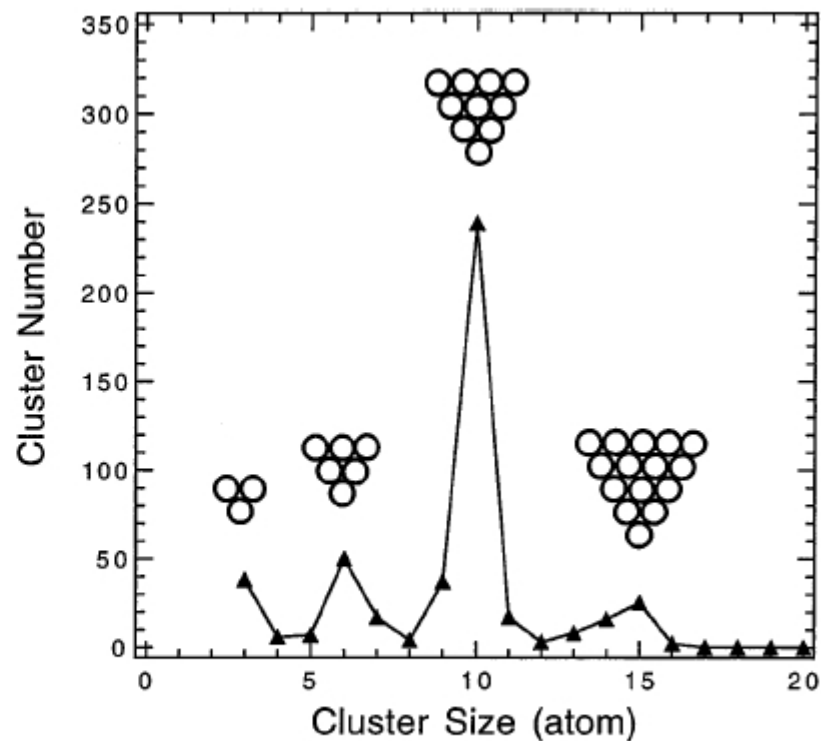


FIG. 2. Histogram of 2D clusters showing the existence of magic numbers.

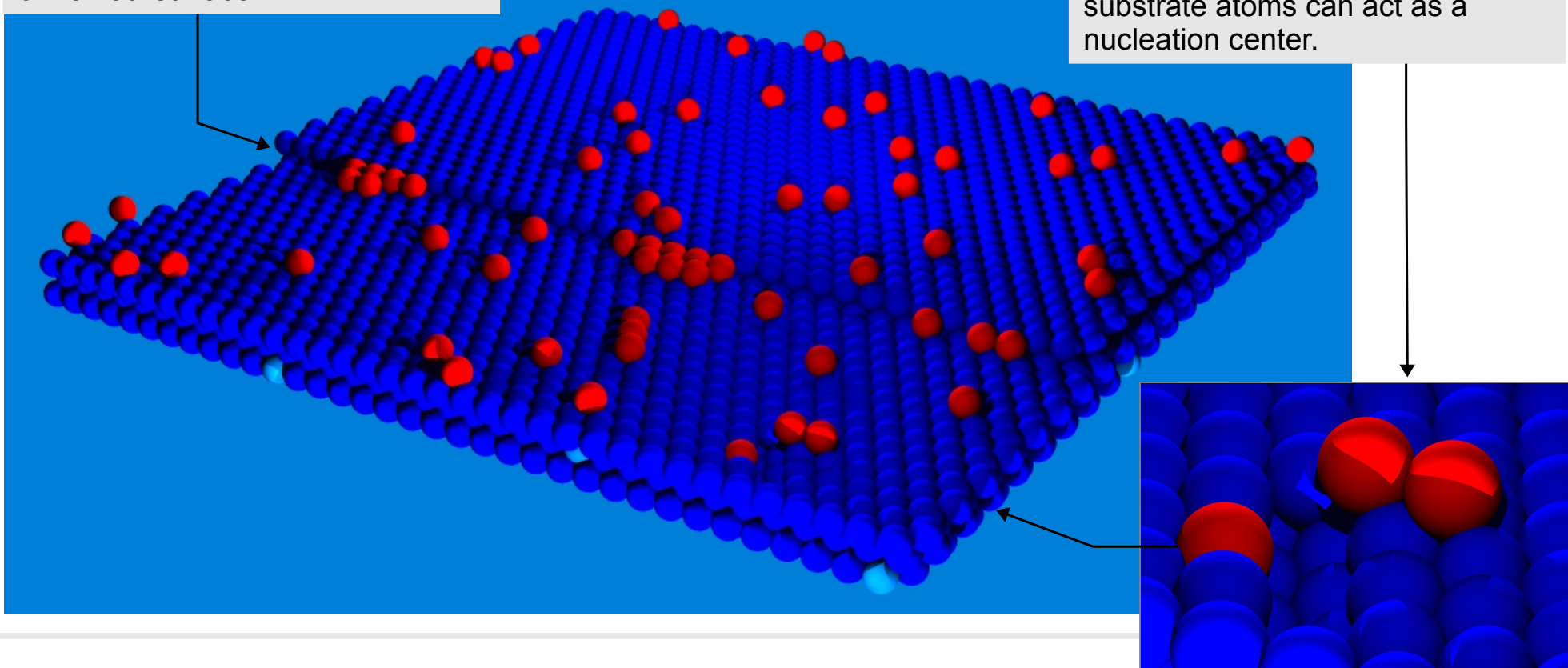
image from: M. Y. Lai, Y. L. Wang, Phys. Rev. Lett **81**, 164 (1998)

# Initial growth

- In practice there are no perfect substrates. There are terraces, broken edges, voids, foreign inclusions and other imperfections present
- The adatom islands often, i.e. more frequently than on “flat” surfaces, nucleate on these imperfections
- At low substrate temperatures and for low density of nucleation centers the probability of an island nucleating away from such center increases – the thermal diffusion is suppressed

An adatom located at the edge of a terrace has more neighbors than on “a flat” surface

Void in a substrate or an island of substrate atoms can act as a nucleation center.



# Initial growth

Vicinal surfaces – in certain applications it is desirable to use surfaces with regular arrangement of terraces which, the surfaces, are obtained by cutting the crystal at low angle relative to low index surfaces

- vicinal substrates can be used for example to deposit regularly spaced nanowires
- the Pt(997) surface – it is the miscut with relative angle  $6.45^\circ$  relative to the (111) surface
- the monoatomic Co chains obtained at nominal thickness of 0.13 ML

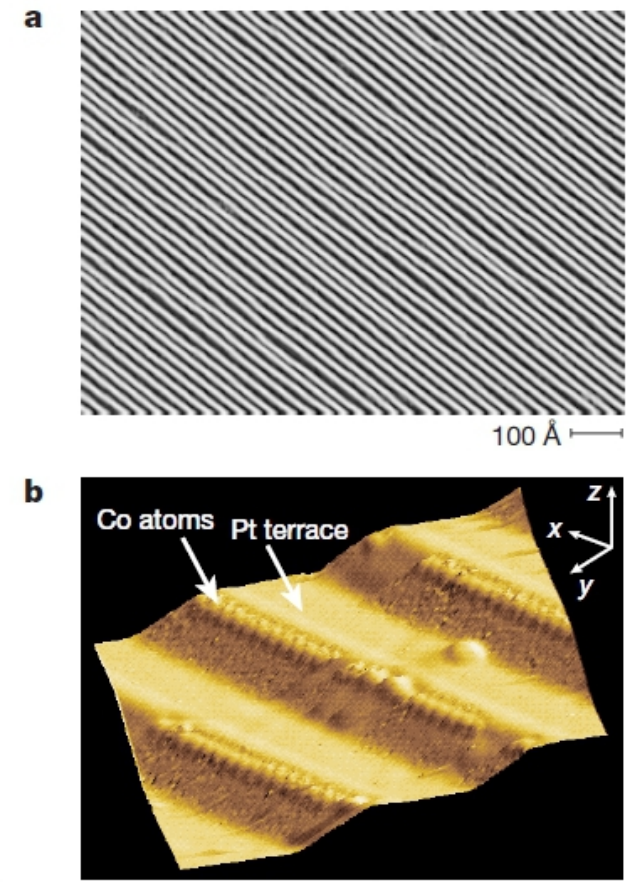


**Figure 1** STM topographs of the Pt(997) surface. **a**, Periodic step structure (each white line represents a single step). The surface has a  $6.45^\circ$  miscut angle relative to the (111) direction; repulsive step interactions result in a narrow terrace width distribution centred at  $20.2 \text{ \AA}$  with  $2.9 \text{ \AA}$  standard deviation. **b**, Co monoatomic chains decorating the Pt step edges (the vertical dimension is enhanced for better contrast). The monoatomic chains are obtained by evaporating 0.13 monolayers of Co onto the substrate held at  $T = 260 \text{ K}$  and previously cleaned by ion sputtering and annealing cycles in ultrahigh vacuum (UHV). The chains are linearly aligned and have a spacing equal to the terrace width.

Reprinted by permission from Macmillan Publishers Ltd: Nature 416, 30, P. Gambardella, A. Dallmeyer, K. Maiti, M. C. Malagoli, W. Eberhardt, K. Kern, C. Carbone, copyright 2002

# Initial growth

In many applications it is useful to artificially introduce defects into the substrate to influence island formation (*guided islanding* [31])

The modifications can be realized by ion bombardment (FIB – focused ion beam) – compare sputtering from the previous lecture

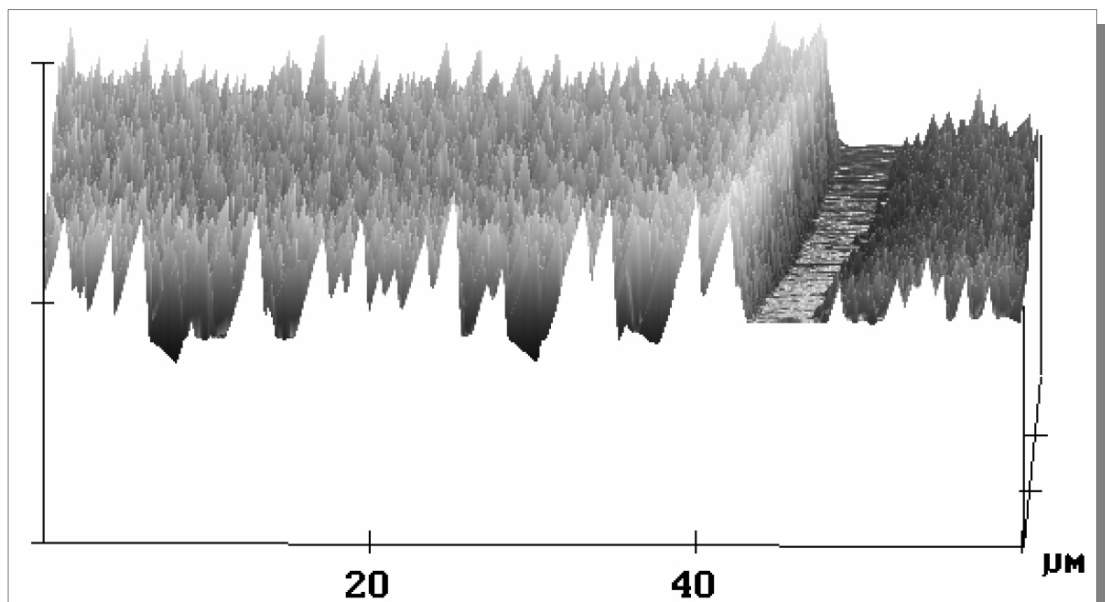


**Figure 4:** Increased island height and number density in the implanted region (left); Normal island growth separated by a few micron wide denuded zone for the untreated region (right).

- 25-30 keV Ga<sup>+</sup> ions
- bombarded areas are characterized by increased island height
- the bombarded areas are separated from untreated regions by denuded zone (the exact structure depends on ion dose)

Here the bombardment is used to create quantum dots\*

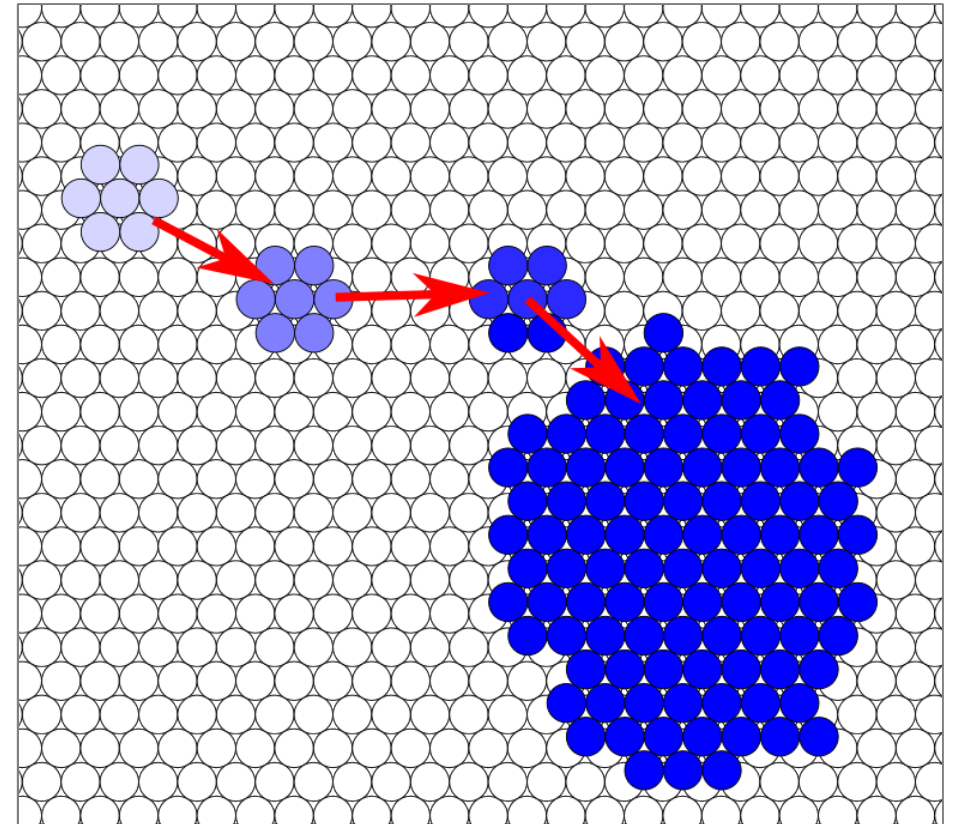
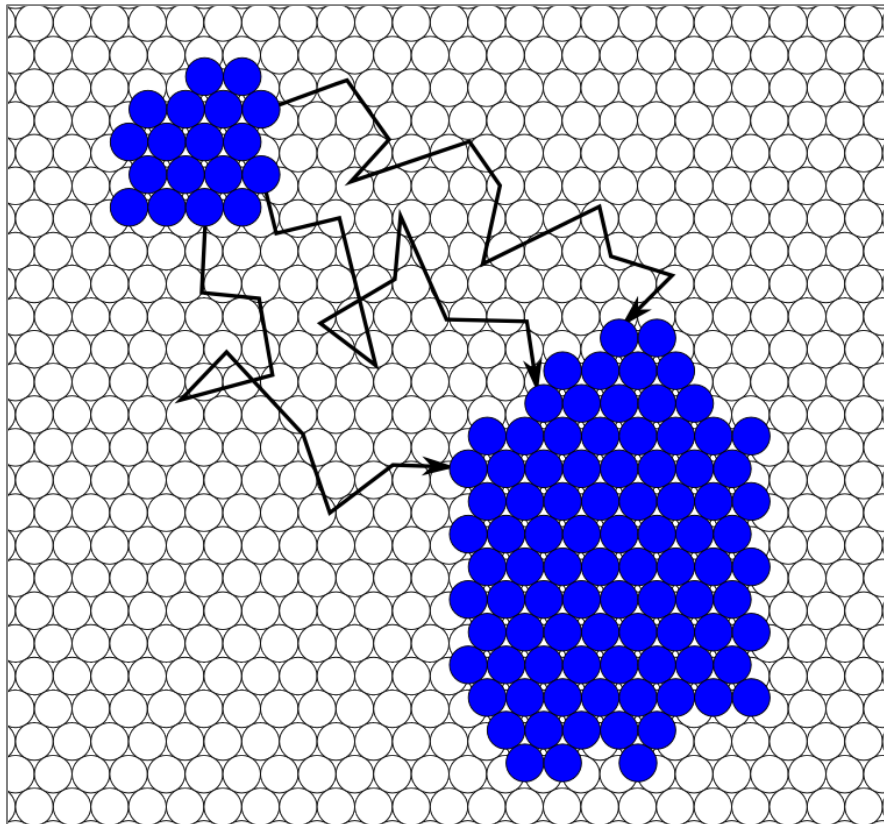
image from: T.E. Vandervelde, S. Atha, T.L. Pernell, R. Hull, J.C. Bean, Mater. Res. Soc. Symposium Proceedings **794**, 111 (2004)

\*"If island dimensions are smaller than the de Broglie wavelength of the charge carrier, they are called quantum dots (Qds)" [31]

# Initial growth

Coarsening – reduction of number of islands [20]:

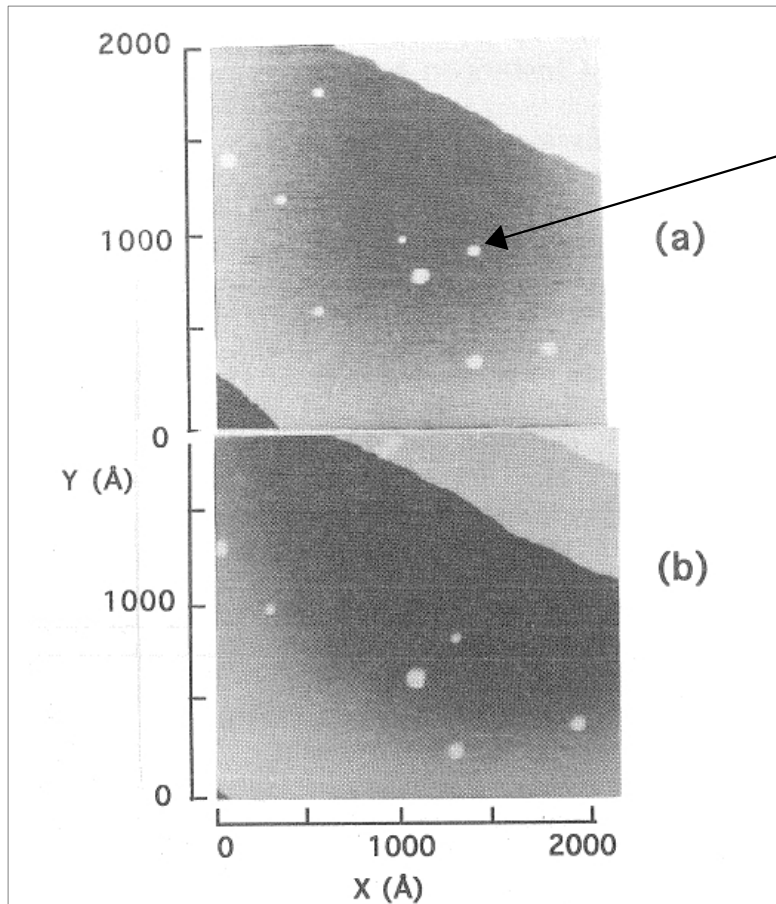
- Ostwald ripening – island dissolution: smaller islands dissolve and feed the growth of larger ones; the process happens mainly for low coverage
- Smoluchowski ripening – islands diffuse to coalesce with other islands



Note that in one system two kinds of ripening can take place depending on a coverage (eg. Ag on Ag (100): Smoluchowski ripening up to approx. 0.65 monolayer [22]).

# Initial growth

## Diffusion of large two-dimensional clusters of Ag on Ag(100)



Ag clusters/islands in the middle of a large terrace

- the individual island encompasses from 100 to 800 atoms ( $8.3$  to  $66.4\text{nm}^2$ )
- the displacement of islands over the period of several hours is of the order of  $10\text{ nm}$
- the motion of clusters is diffusive for long time between observations
- diffusion coefficients for the center of mass of large clusters (above  $30\text{nm}$ ) are of the order of  $1 \times 10^{-21}\text{ m}^2\text{s}^{-1}$

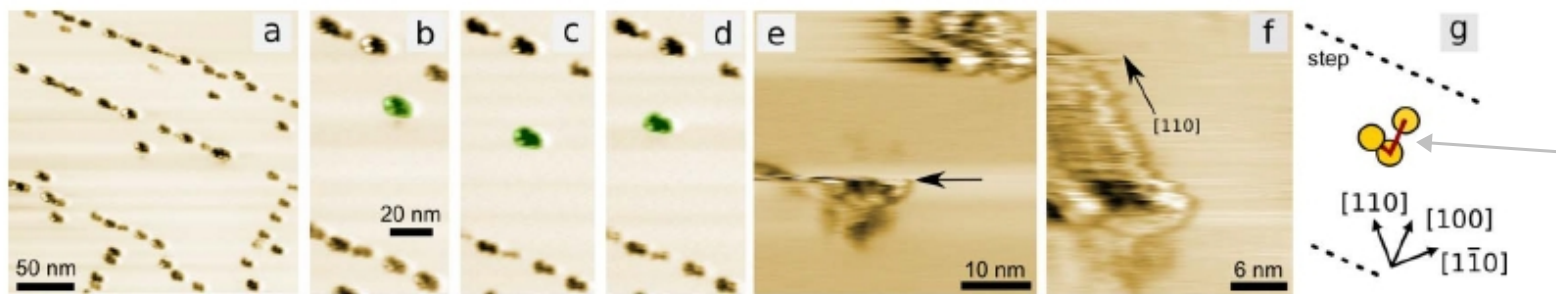
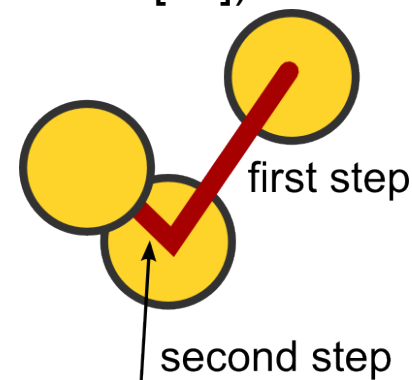
FIG. 1. STM images obtained following deposition of  $0.007$  monolayers (ML) Ag on Ag(100) at room temperature. The deposition rate is  $4 \times 10^{-3}$  ML/s. (a)  $t = 0$  h. (b)  $t = 5.7$  h. Contamination at step edge is most apparent in (b).

image source: J.-M. Wen, S.-L. Chang, J.W. Burnett, J.W. Evans, P. A. Thiel, Phys. Rev. Lett **73**, 2591 (1994)

# Initial growth

A small digression - manipulation of nanoclusters

- strong cohesion within the clusters (i.e. they do not wet the substrate [25]) enables us to move the whole clusters with AFM tips [24]
- Au clusters on NaCl(001); RT
- cluster size approx. 5 nm (~2500 atoms)
- first manipulation step – 16 nm; the second step – 11 nm



**Figure 2 | Manipulation of a Au cluster (green) on NaCl(001) along the [110] and [100] directions (nominal Au thickness: 0.3 mono-layers, flux:  $4.1 \times 10^{12}$  atoms/cm<sup>2</sup>/s). (a) The surface region before the manipulation (density:  $0.9 \times 10^{11}$  clusters/cm<sup>2</sup>, cluster-cluster mean distance at steps:  $\sim 20$  nm). (b)–(d) The cluster before (b), after the first (c) and after the second (d) manipulation experiment. (e) During the first manipulation, a part of the cluster could be still imaged until the position labeled by the arrow where the cluster suddenly started to escape behind the tip (*backheel*). (f) During the second manipulation step, the cluster was moved by sliding along the [110] direction. (g) Schematic of the two manipulation steps. (a)  $250 \times 250$  nm<sup>2</sup>,  $\Delta f = -22$  Hz, (b, c, d)  $65 \times 136$  nm<sup>2</sup>,  $\Delta f \approx -22; -18; -20$  Hz, (e)  $40 \times 40$  nm<sup>2</sup>,  $\Delta f = -48$  Hz, (f)  $30 \times 26$  nm<sup>2</sup>,  $\Delta f = -69$  Hz, All images:  $f_0 = 275$  kHz,  $v_{scan} = 10$  Hz (e: 24 Hz, f: 33 Hz),  $k = 28$  N/m,  $A_{pp} = 15$  nm.**

# Initial growth

## Mound formation [18,20]

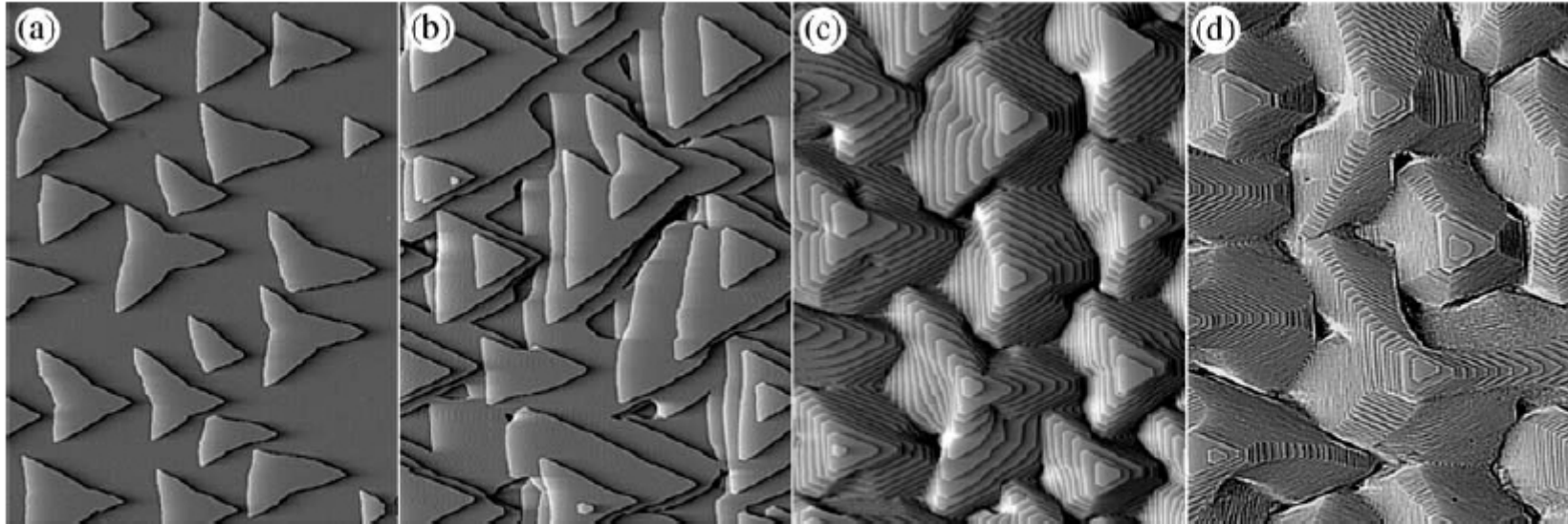


Fig. 2. Growth of Pt on Pt(111) at  $T=440$  K [5]. The total coverage is (a) 0.3 monolayers (ML), (b) 3 ML, (c) 12 ML and (d) 90 ML. The image size is  $2600 \text{ \AA} \times 3450 \text{ \AA}$ . Courtesy of T. Michely.

image from: J. Krug, Physica A 313, 47 (2002)

- Ehrlich-Schwoebel barrier suppresses interlayer diffusion – adatom which lands on a given layer is likely to remain there
- If the barrier is sufficiently strong mound pattern develops

# Initial growth

## Coalescence of islands [4, 26]

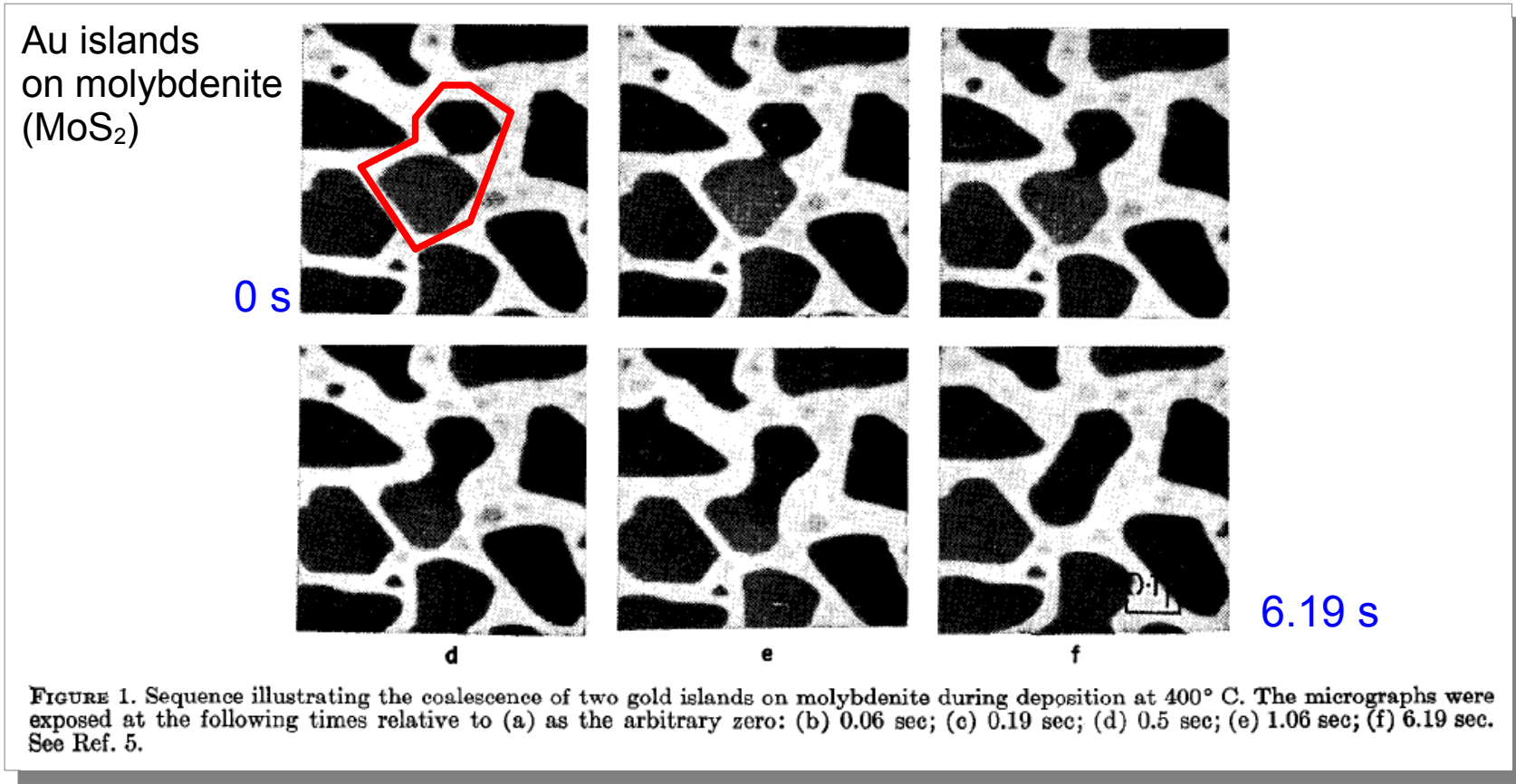
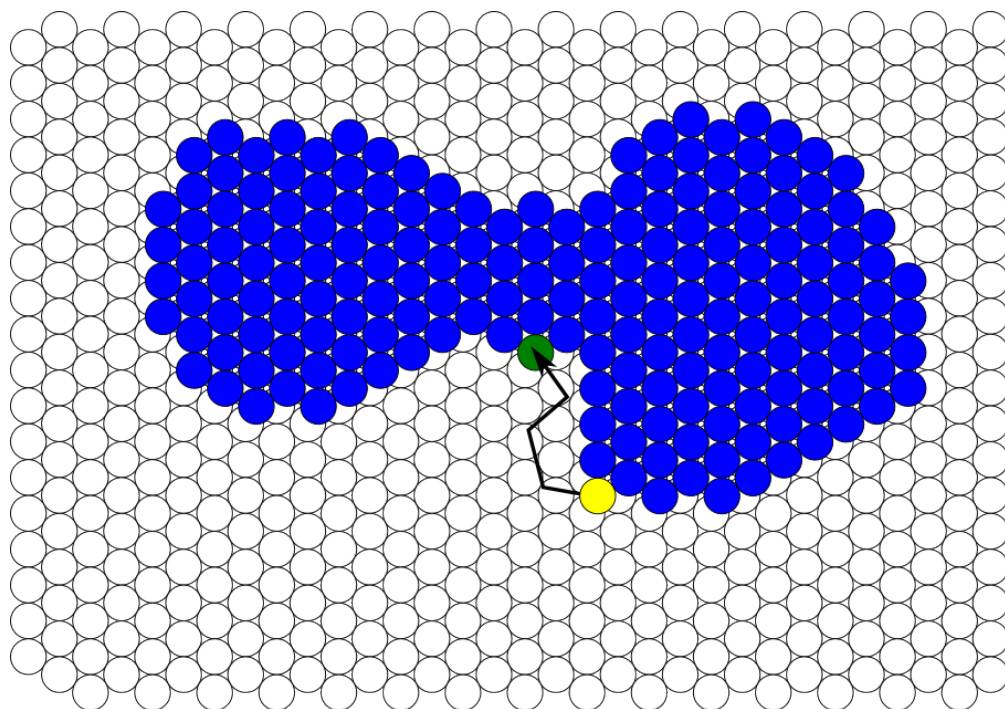


image from: D.W. Pashley, M.J. Stowell,  
J. Vac. Sci. Technol. **3**, 156 (1966)

- the driving force for neck growth is lower energy of the molecules in the concave neck [4]
- the mass transport into the neck joins the islands: the neck [panel (b)] was formed within 0.06s !

# Initial growth

## Coalescence of islands [4, 26]



Free sites in the narrowing on average offer more neighbors

Atom moving from low coordinated yellow site to green site gains one neighbor diminishing potential energy of the island

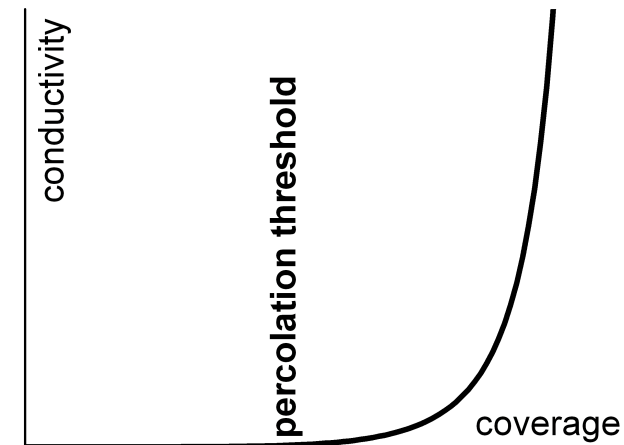
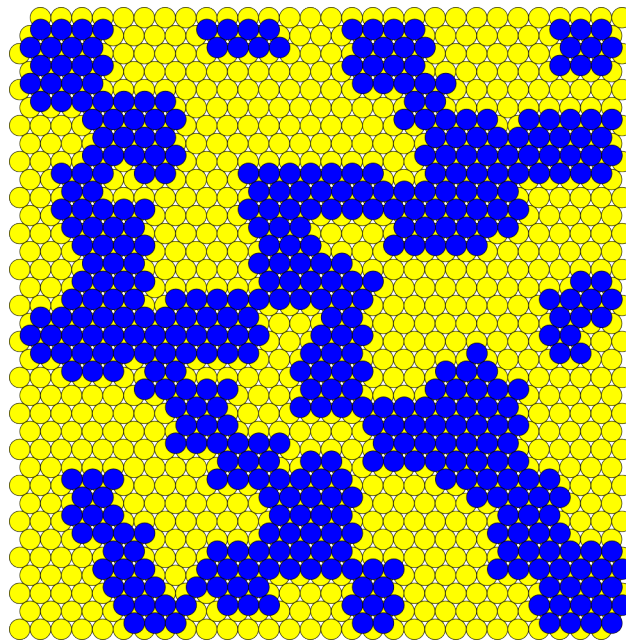
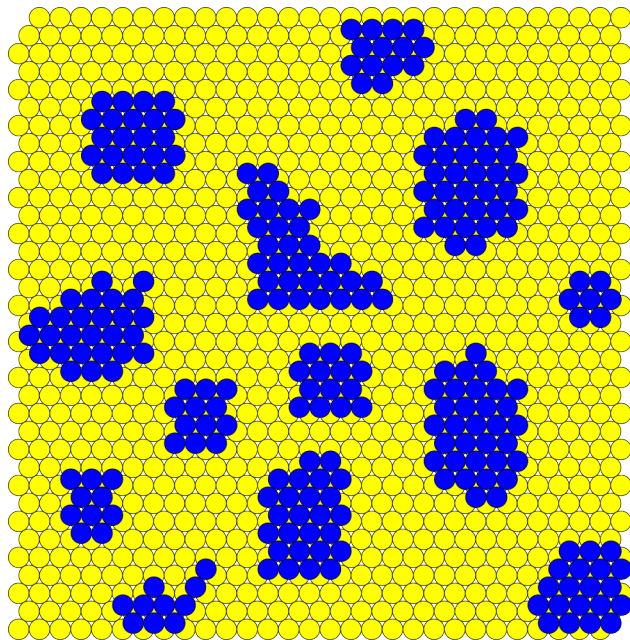
- the driving force for neck growth is lower energy of the molecules in the concave neck [4]

# Initial growth

Percolation – at certain stage of thin film deposition the layer becomes continuous on a macroscopic scale

There are different physical quantities which may display the phenomenon of percolation:

- the film may become geometrically continuous – the islands are in contact and the film as a whole becomes conductive
- the film may develop magnetic continuity – although the islands do not necessarily percolate from geometrical point of view; the magnetostatic interactions may extend over the whole film



# Initial growth

the film may develop magnetic continuity although the islands do not necessarily percolate from geometrical point of view the magnetostatic interactions may extend over the whole film:

- $15 \pm 2$  nm Co particles deposited on carbon substrate by evaporation of a colloid
- the particles are separated by at least 2 nm (oleic acid surfactant thickness)
- long range magnetic order develops in disordered assembly
- off-axis electron holography is used to map directly the in plane magnetic field
- the field is used then to “*estimate the magnitude and orientation of the magnetic moment of each individual particle*”

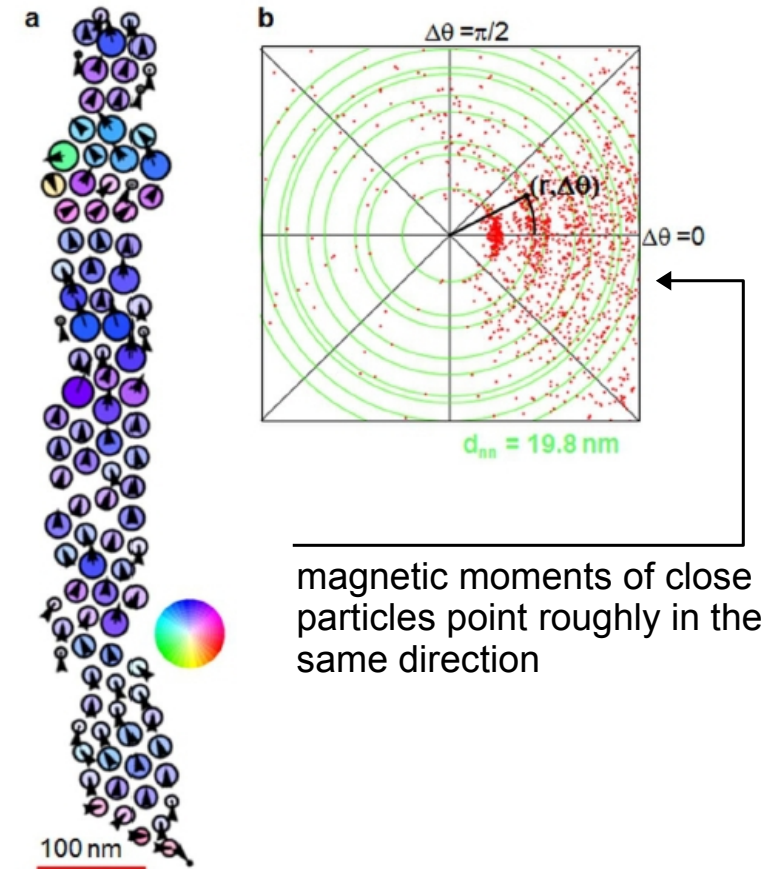


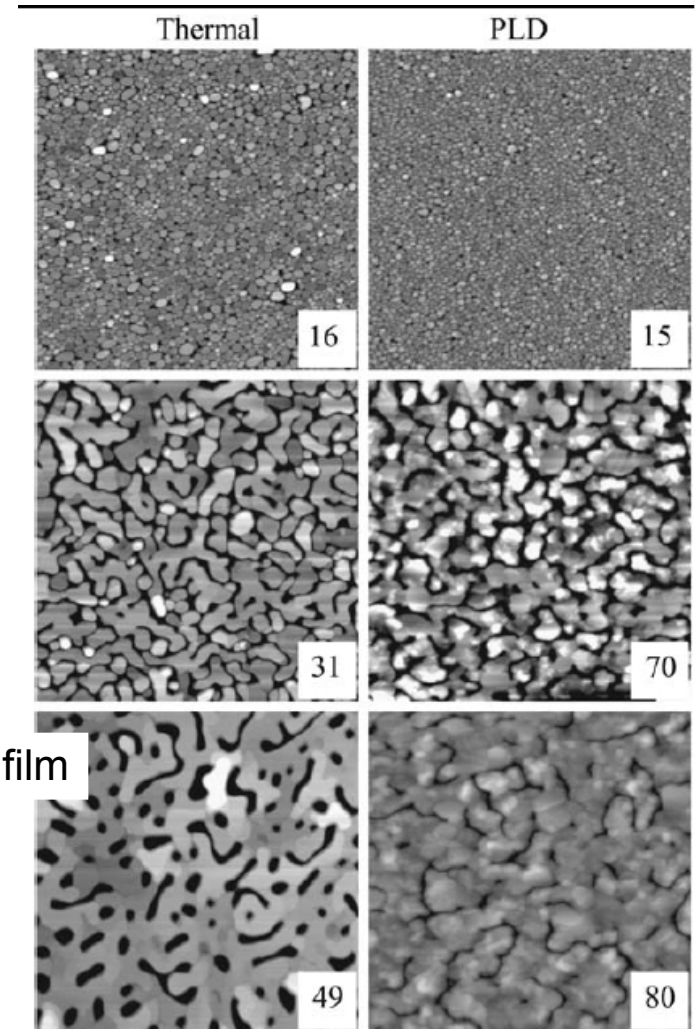
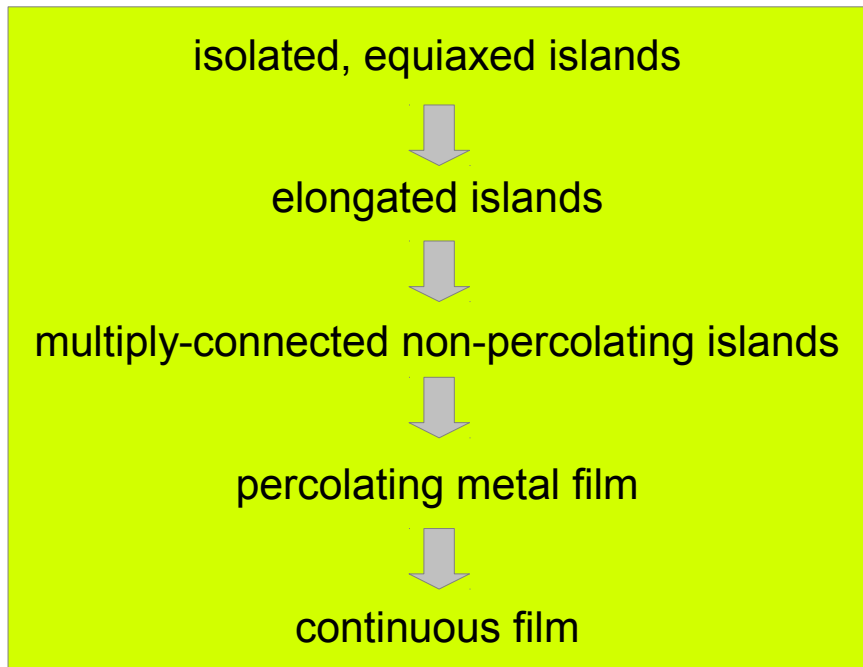
Figure 4 | Results obtained from measurement of chain IV in Fig. 3. (a) Estimated magnetic moment distribution, (b) radial-angular ( $r, \Delta\theta$ ) distribution function, where  $r$  is distance between two magnetic moments (particle centers) and  $\Delta\theta$  is the angular difference in their moment orientations, measured for all pairs of moments in the chain. The thin green circular lines superimposed on (b) indicate the expected locations of the first few neighbouring peaks for a 2D close-packed lattice with a measured nearest neighbour distance  $d_{nn}$  of 19.8 nm.

image from: M. Varon, M. Beleggia, T. Kasama, R.J. Harrison, R.E. Dunin-Borkowski, V.F. Puntès, C. Frandsen, *Sci. Rep.* **3**, 1234 (2013)

# Initial growth

Percolation – at certain stage of thin film deposition the layer becomes continuous on macroscopic scale.

*“As shown in Fig. 3, in metal-on-insulator film growth the morphology evolution is characterized by a transition from isolated, equiaxed\* islands to elongated islands to multiply-connected non-percolating islands to a percolating metal film to the filling in of holes.” [27]*



**Fig. 3** Metal-on-insulator Volmer–Weber growth mode, illustrating transition from equiaxed islands (top row) to extended, non-percolating islands (middle row) to a percolating metal film with holes filling in (bottom row). Ag on mica; scan edge length is 5  $\mu\text{m}$ . Inset is average film thickness. Adapted from [49]

image from: M.J. Aziz, Appl. Phys. A **93**, 579 (2008)

\*equiaxed - having approximately equal dimensions in all directions —used esp. of a crystal grain in a metal [28 -www.merriam-webster.com]

# Further stages of film growth

After reaching the substrate the atom (becoming adatom) diffuses to “equilibrium” position and becomes incorporated into the film (some atoms may desorb back to vapor)

- Depending on various factors (temperature, pressure, deposition method, etc.) the thick film may develop into single crystal or more probably into a polycrystalline or amorphous structure
- After initial stages of islands/crystal formation the large islands become fixed in position (they no longer diffuse over the surface)
- The islands/crystals may have different crystallographic orientation [34]
- “*The island with lower energy per atom consumes the other(s), resulting in a new single-crystal island as the system attempts to minimize the overall surface and interface energy.*” I. Petrove *et al.* [33]

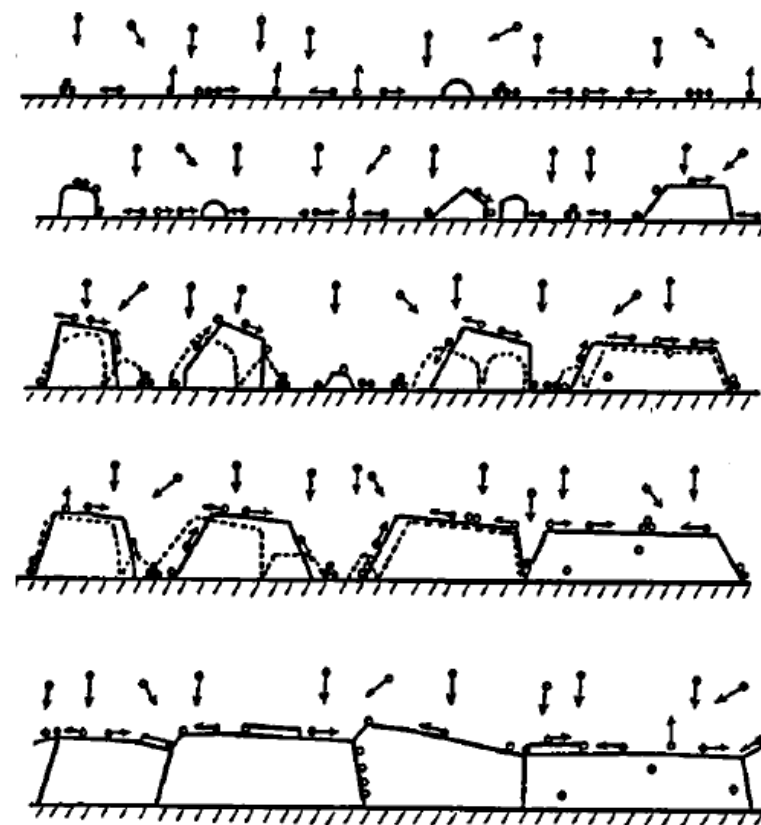


FIG. 1. Schematic diagram illustrating fundamental growth processes controlling microstructural evolution: nucleation, island growth, impingement and coalescence of islands, grain coarsening, formation of polycrystalline islands and channels, development of a continuous structure, and film growth (see Ref. 9).

# Further stages of film growth

- Usually the densest **planes of crystals grow fastest** as they offer higher potential energy decrease as a result of incorporation of an adatom (in other word the low-diffusivity surfaces grow faster – higher bonding energy restricts diffusion)\*

For common structures the planes are [33]:

(111) for fcc

(0002) for hcp

(110) for bcc

- the faster growing crystals that grow at the cost of other develop into V-shaped forms [34]
- when film reaches certain thickness only grains of one orientation proceed to the free surface [34]

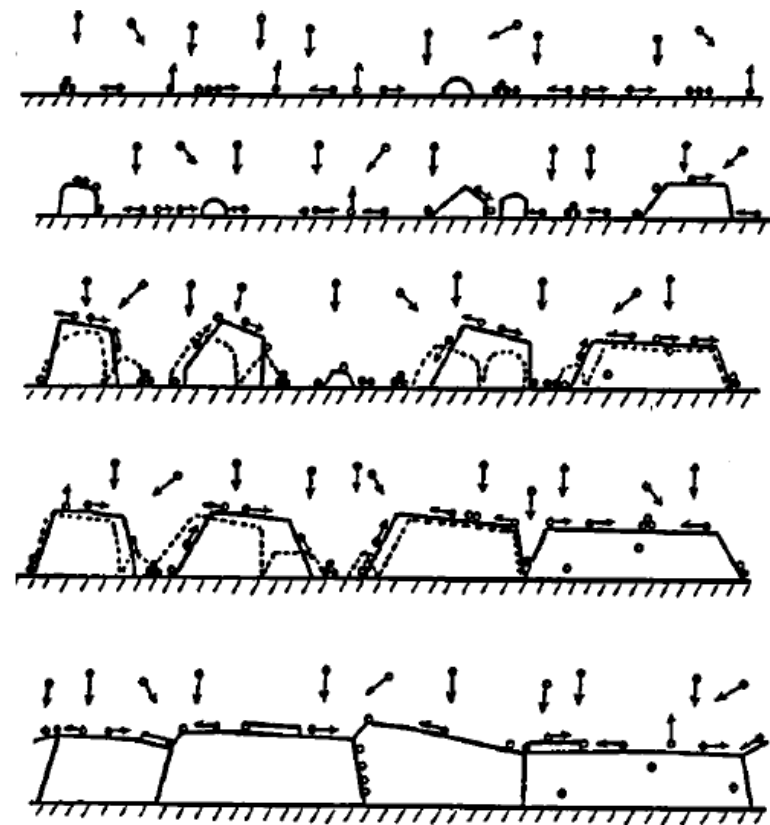


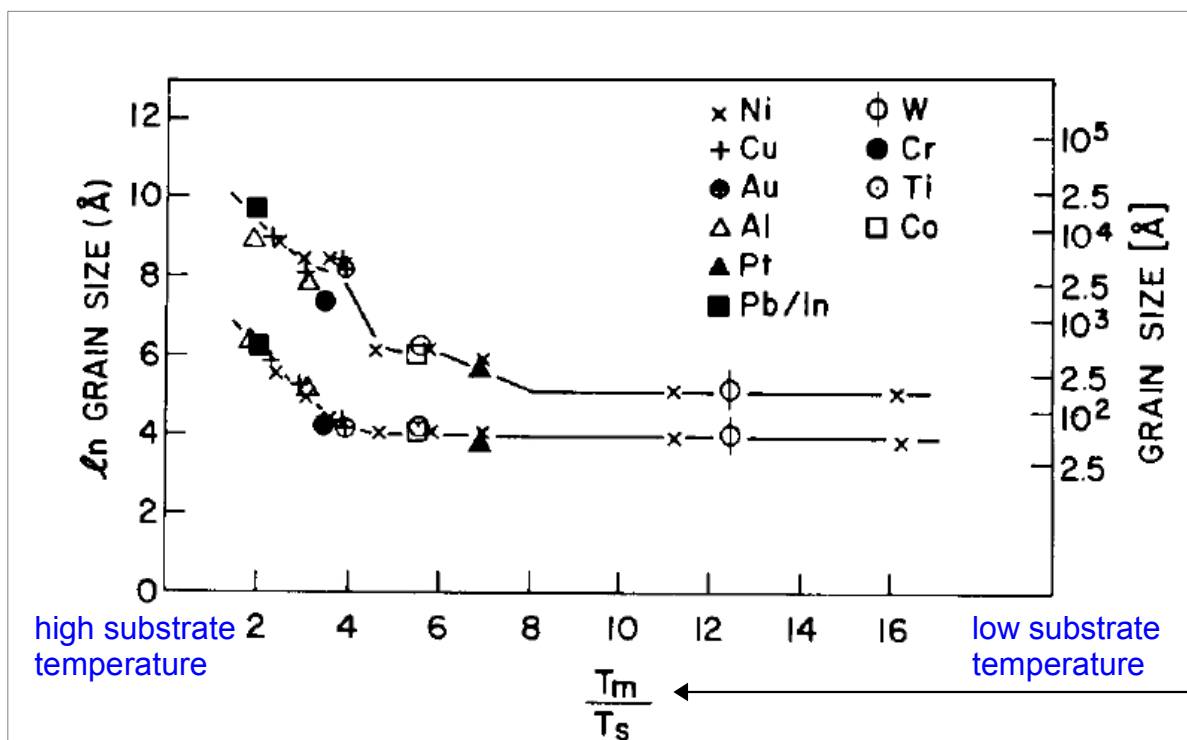
FIG. 1. Schematic diagram illustrating fundamental growth processes controlling microstructural evolution: nucleation, island growth, impingement and coalescence of islands, grain coarsening, formation of polycrystalline islands and channels, development of a continuous structure, and film growth (see Ref. 9).

image from: I. Petrov, P.B. Barna, L. Hultman, J.E. Greene, J. Vac. Sci. Technol. A **21**, S117 (2003)

\*for Monte-Carlo simulations of columnar growth see Ref. [35]: G.H. Gilmer et al., Thin Solid Films **365**, 189 (2000)

# Further stages of film growth

The diffusion is to much extent controlled by the substrate temperature,  $T_s$ .  
 The diffusion on the other hand is characterized by activation energy which scales directly with the melting point  $T_m$  of the condensate [4]  
 The dependence  $[D(T_s) \rightarrow D(T_s/T_m)]$ , compare slide 18] is the basis of a zone structure models which have been developed to describe structure of films at later stages of growth [4,35].



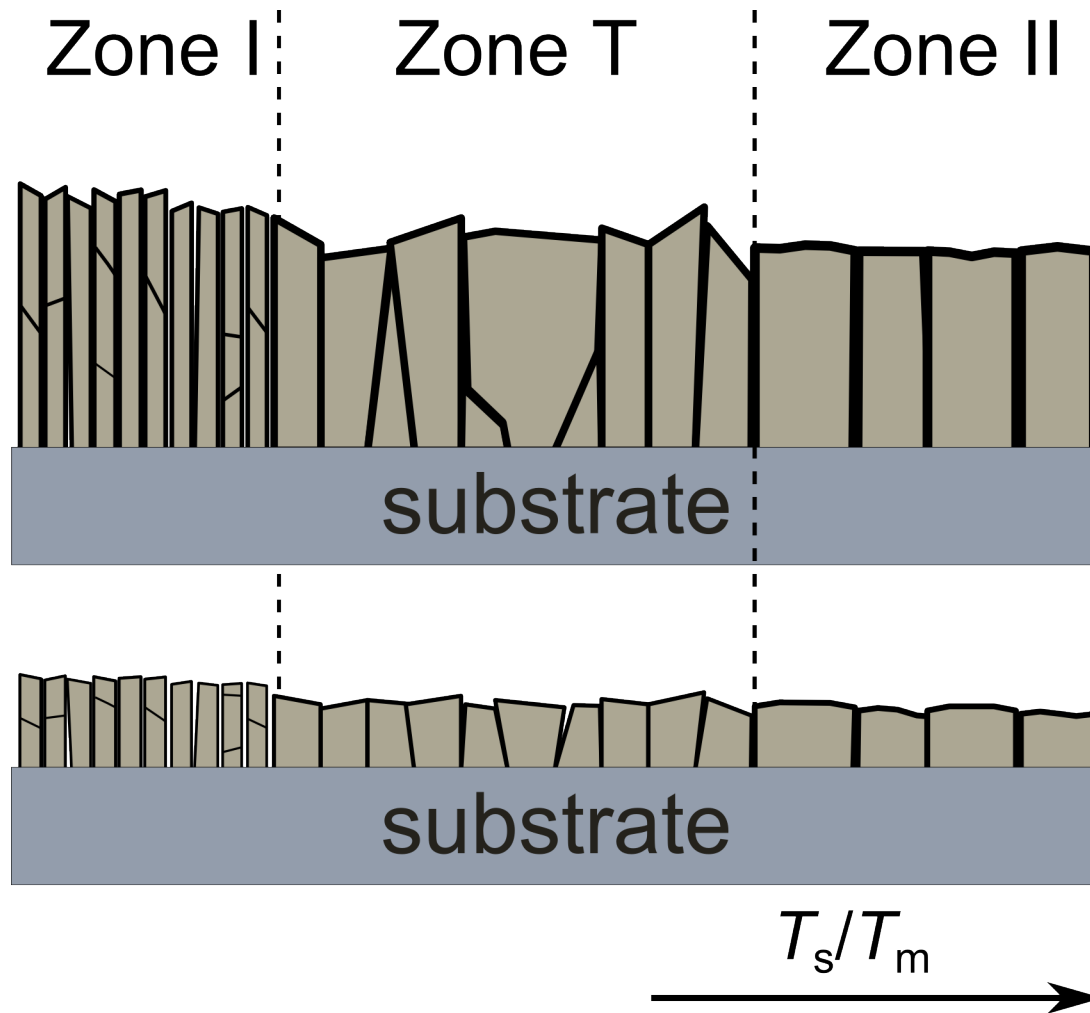
- electron beam evaporated structures
- thickness – 100nm
- grains are larger for higher substrate temperature – enhanced diffusion

FIG. 1. A plot of maximum and minimum grain size variation with homologous substrate temperature for thin films of ten different metals.

note that abscissa is proportional to an inverse of  $T_s$

# Further stages of film growth

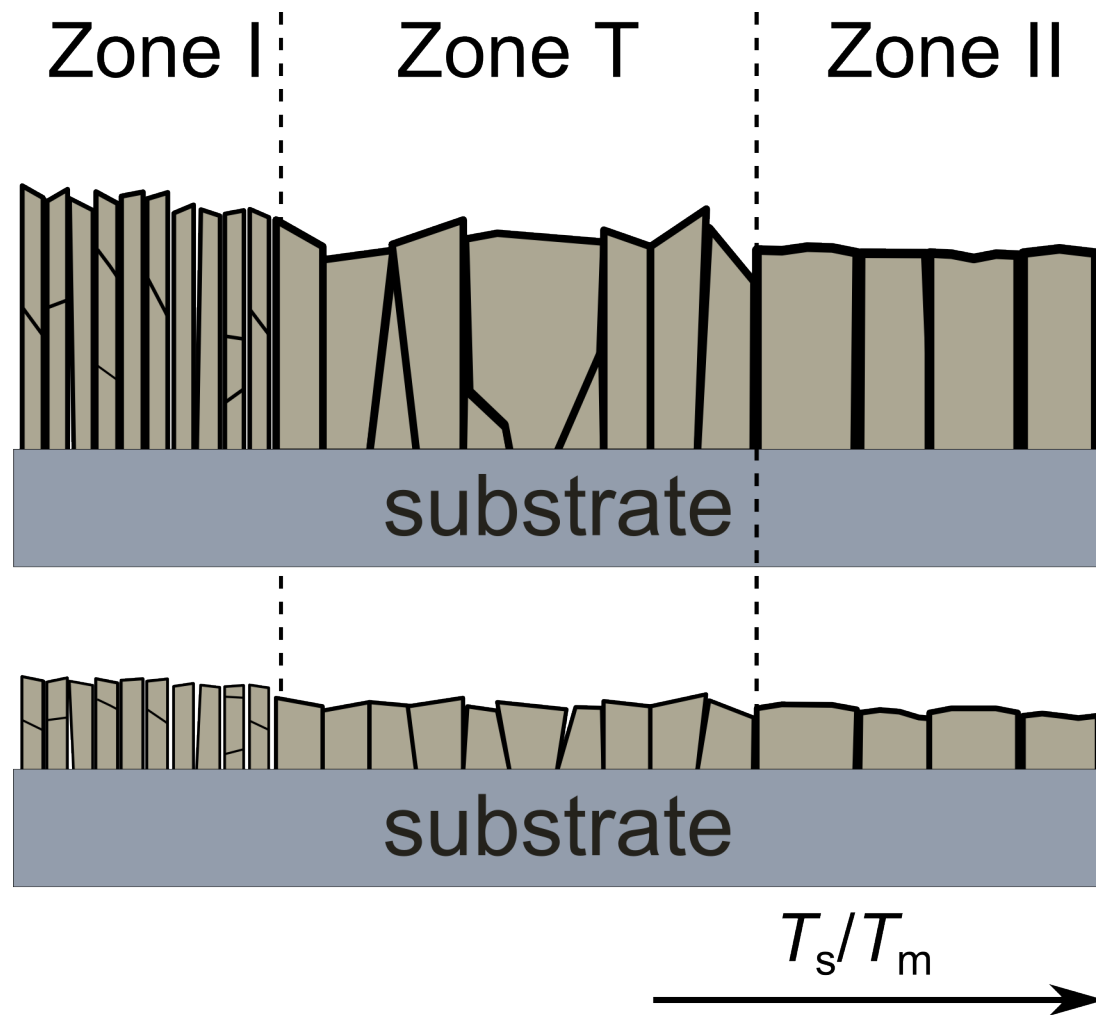
Exemplary zone model for pure elemental films (according to Refs. 4, 33)



- **Zone I** ( $T_s/T_m < 0.2$ ): very low deposition temperatures and thus negligible surface diffusion (virtually no bulk diffusion), fiber texture develops, orientation of columns random (preserves the orientation of nuclei), the individual columns are usually composed of grains of different orientation
- **Zone T** – surface diffusion becomes important, smaller grains coalesce or their atoms are incorporated into larger, energetically more favorable grains. *“The consequence of competitive growth is a continuous change in morphology, texture, and surface topography (and, hence, film properties!) as a function of film thickness. Near the substrate, the microstructure consists of randomly oriented small grains out of which V-shaped columns with the favored orientations slowly emerge and overgrow kinetically disadvantaged columns. This gives rise to increased preferred orientation.”* - I. Petrov et al. [33]

# Further stages of film growth

Exemplary zone model for pure elemental films (according to Refs. 4, 33)



- Zone II** – bulk diffusion becomes important, grain boundary diffusion which at lower deposition temperatures was active only in coalescence stage is present during the whole thickening process; large grains grow at the expense of smaller or unfavorably oriented ones; recrystallization takes place which can lead to change of grain size distribution from monomodal\* to bimodal and again to monomodal – in-plane sizes of grains become much larger and the surface of the films smoothens.

image based on Fig.3 from Ref [33]: I. Petrov, P.B. Barna, L. Hultman, J.E. Greene, J. Vac. Sci. Technol. A **21**, S117 (2003)

\*one size strongly dominates the distribution

# Further stages of film growth

## Examples of columnar growth

ZnO nanostructures obtained with metal-organic chemical vapor deposition (MOCVD)

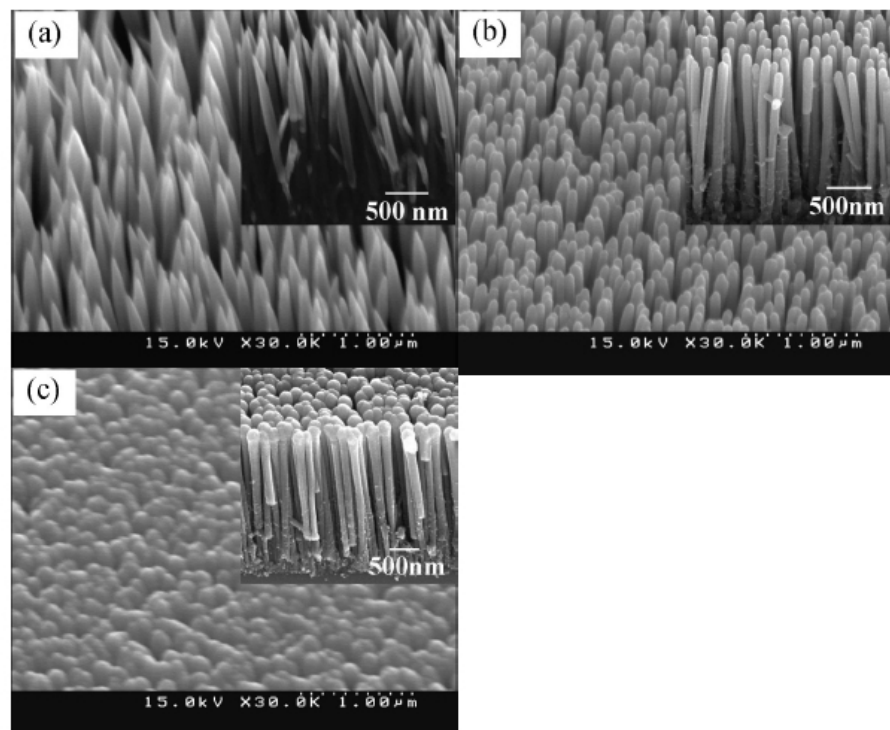


**Figure 1.** Surface morphologies of vertically aligned ZnO nanowires: (a) nanoneedles, (b) nanonails and (c) nanowires with rounded tip.

image from: S. Nath Das, J. Prakash Kar, J. Xiong, J-M Myoung, Chapter 2 in "Nanowires - Recent Advances", ed. by Xihong Peng, ISBN 978-953-51-0898-6 (2012)

# Bibliography

- [1] wikipedia.org
- [2] "Silicon Wafers Production Specifications Si and SiO<sub>2</sub> Etching Our Portfolio", [http://www.microchemicals.eu/pdf/silicon\\_wafers.pdf](http://www.microchemicals.eu/pdf/silicon_wafers.pdf)
- [3] An Introduction to Surface Chemistry, R.M. Nix, <http://www.chem.qmul.ac.uk/surfaces/scc/>
- [4] M. Ohring, The materials science of thin films, Academic Press Inc., 1992
- [5] R.V. Stuart, G.K. Wehner, J. Appl. Phys. **35**, 1819 (1964)
- [6] H. Ibach, Physics of Surfaces and Interfaces, Springer-Verlag Berlin Heidelberg 2006
- [7] G. Antczak, G. Ehrlich, Surface Science Reports 62, **39** (2007)
- [8] L.I. Maissel, R. Glang, Handbook of Thin Film Technology, McGraw-Hill, New York 1970
- [9] M. Hohage, M. Bott, M. Morgenstern, Z. Zhang, T. Michely, G. Comsa, Phys. Rev. Lett. **76**, 2366 (1996)
- [10] M. Einax, W. Dieterich, P. Maass, Rev. Mod. Phys. **85**, 921 (2013)
- [11] S. Ogura, K. Fukutani, M. Matsumoto, T. Okano, M. Okada, T. Kawamura, Phys. Rev. B **73**, 125442 (2006)
- [12] F.F. Leal, S.C. Ferreira, S.O. Ferreira, J. Phys. Condens. Matter **23**, 292201 (2011)
- [13] S.J. Liu, E.G. Wang, C.H. Woo, H. Huang, Journal of Computer-Aided Materials Design **7**, 195 (2001)
- [14] M.A. Herman, W. Richter, H. Sitter, Epitaxy: Physical principles and technical implementation, Springer 2004
- [15] A.V. Ramos, J.-B. Moussy, M.-J. Guittet, M. Gautier-Soyer, C. Gatel, P. Bayle-Guillemaud, B. Warot-Fonrose, E. Snoeck, Phys. Rev. B **75**, 224421 (2007)
- [16] M. Y. Lai, Y. L. Wang, Phys. Rev. Lett **81**, 164 (1998)
- [17] D. Jaworski, A. Dietaław, L. Milkowska, G. Siergiejew, Kurs Fizyki Tom.1, Mechanika..., PWN Warszawa 1981
- [18] J. Krug, Physica A **313**, 47 (2002)
- [19] I. Berbezier, A. Karmous, A. Ronda, A. Sgarlata, A. Balzarotti, P. Castrucci, M. Scarselli, M. De Crescenzi, Appl. Phys. Lett. **89**, 063122 (2006)
- [20] J.W. Evans, P.A. Thiel, M.C. Bartelt, Surface Science Reports **61**, 1 (2006)
- [21] K. Morgenstern, G. Rosenfeld, G. Comsa, Phys. Rev. Lett **76**, 2113 (1996)
- [22] J.-M. Wen, J.W. Evans, M.C. Bartelt, J.W. Burnett, and P.A. Thiel, Phys. Rev. Lett **76**, 652 (1996)
- [23] J.-M. Wen, S.-L. Chang, J.W. Burnett, J.W. Evans, and P. A. Thiel, Phys. Rev. Lett **73**, 2591 (1994)
- [24] T. Hynninen, G. Cabailh, A.S. Foster, C. Barth, Scientific Reports **3**, 1270 (2013)
- [25] J.A Venables, G.D.T Spiller, M. Hanbücken, Rep. Prog. Phys. **47**, 399 (1984)
- [26] D.W. Pashley, M.J. Stowell, J. Vac. Sci. Technol. **3**, 156 (1966)
- [27] M.J. Aziz, Appl. Phys. A **93**, 579 (2008)

# Bibliography

- [28] <http://www.merriam-webster.com>
- [29] M. Varon, M. Beleggia, T. Kasama, R.J. Harrison, R.E. Dunin-Borkowski, V.F. Puentes, C. Frandsen, *Sci. Rep.* **3**, 1234 (2013)
- [30] H-P Cheng , U. Landman, *J. Phys. Chem.* **98**, 3527 (1994)
- [31] T.E. Vandervelde, S. Atha, T.L. Pernel, R. Hull, J.C. Bean, *Mater. Res. Soc. Symposium Proceedings* **794**, 111 (2004)
- [32] J.C. Bean, *Proceedings of the IEEE* **80**, 571 (1992)
- [33] I. Petrov, P.B. Barna, L. Hultman, J.E. Greene, *J. Vac. Sci. Technol. A* **21**, S117 (2003)
- [34] P.B. Barna, M. Adamik, *Thin Solid Films* **317**, 27 (1998)
- [35] G.H. Gilmer, H. Huang, T. D. de la Rubia, J. Dalla Torre, F. Baumann, *Thin Solid Films* **365**, 189 (2000)
- [36] P. Gambardella, A. Dallmeyer, K. Maiti, M. C. Malagoli, W. Eberhardt, K. Kern, C. Carbone, *Nature* **416**, 30 (2002)
- [37] H. T. G. Hentzell , C. R. M. Grovenor and D. A. Smith, *J. Vac. Sci. Technol. A* **2**, 218 (1984)
- [38] S. Nath Das, J. Prakash Kar, J. Xiong, J-M Myoung, Chapter 2 in "Nanowires - Recent Advances" , edited by Xihong Peng, ISBN 978-953-51-0898-6 (2012)
- [39] D. Kashchiev, *Basic Results and Applications of Nucleation Theory* ([www.emse.fr/fr/transfert/spin/trs/pdf/nucleation/lecture1.pdf](http://www.emse.fr/fr/transfert/spin/trs/pdf/nucleation/lecture1.pdf), retrieved on 2014.04.01)
- [40] B. Bhushan (ed.), *Encyclopedia of Nanotechnology*, Springer 2012

# Acknowledgment

During the preparation of this, and other lectures in the series “*Magnetic materials in nanoelectronics – properties and fabrication*” I made an extensive use of the following software for which I wish to express my gratitude to the authors of these very useful tools:

- OpenOffice [www.openoffice.org](http://www.openoffice.org)
- Inkscape [inkscape.org](http://inkscape.org)
- POV-Ray [www.povray.org](http://www.povray.org)
- Blender [www.blender.org](http://www.blender.org)
- SketchUp [sketchup.com.pl](http://sketchup.com.pl)

I also used “Fizyczne metody osadzania cienkich warstw i metody analizy powierzchniowej” lectures by Prof. F. Stobiecki which he held at Poznań University of Technology in 2011.